Available online at www.sciencedirect.com
ScienceDirect
J. Differential Equations 246 (2009) 552–580
Journal of Differential Equations
www.elsevier.com/locate/jde

Spatial complexity in multi-layer cellular neural networks

Jung-Chao Ban [a], Chih-Hung Chang [b], Song-Sun Lin [b,*], Yin-Heng Lin [c]

[a] *Department of Mathematics, National Hualien University of Education, 97063 Hualien, Taiwan, ROC*
[b] *Department of Applied Mathematics, National Chaio-Tung University, 30050 Hsinchu, Taiwan, ROC*
[c] *Department of Mathematics, National Central University, 32054 Chung-Li, Taiwan, ROC*

Received 26 February 2008; revised 7 May 2008

Available online 4 June 2008

Abstract

This study investigates the complexity of the global set of output patterns for one-dimensional multi-layer cellular neural networks with input. Applying labeling to the output space produces a sofic shift space. Two invariants, namely spatial entropy and dynamical zeta function, can be exactly computed by studying the induced sofic shift space. This study gives sofic shift a realization through a realistic model. Furthermore, a new phenomenon, the broken of symmetry of entropy, is discovered in multi-layer cellular neural networks with input.

MSC: 37A35; 37B10; 37B15; 37B40; 37C30

Keywords: Cellular neural networks; Sofic shift; Spatial entropy; Dynamical zeta function

1. Introduction

The cellular neural network (CNN) proposed by Chua and Yang is a large aggregate of analogue circuits [8,9]. The system presents itself as an array of identical cells which are all locally coupled. Many such systems have been studied as models for spatial pattern formation in biology [10–12,16,17], chemistry [13], physics [6], image processing and pattern recognition [7].

* Corresponding author.
E-mail addresses: jcban@mail.nhlue.edu.tw (J.-C. Ban), grece.am92g@nctu.edu.tw (C.-H. Chang), sslin@math.nctu.edu.tw (S.-S. Lin), yhlin@math.ncu.edu.tw (Y.-H. Lin).

0022-0396/$ – see front matter
doi:10.1016/j.jde.2008.05.004

The complexity of the set of global patterns for one- or two-dimensional cellular neural networks has been widely discussed [1–5,14,15,19]. However, this study is the first to explore the complexity for one-dimensional multi-layer CNN. The two-dimensional sofic and two-dimensional multi-layer CNN are discussed in other papers.

A one-dimensional multi-layer CNN system with input is realized as the following form,

$$\frac{dx_i^{(n)}}{dt} = -x_i^{(n)} + \sum_{|k|\leqslant d} a_k^{(n)} y_{i+k}^{(n)} + \sum_{|k|\leqslant d} b_k^{(n)} u_{i+k}^{(n)} + z^{(n)}, \tag{1.1}$$

for some $d \in \mathbb{N}$, $1 \leqslant n \leqslant N \in \mathbb{N}$, $i \in \mathbb{Z}$, where

$$u_i^{(n)} = y_i^{(n-1)} \quad \text{for } 2 \leqslant n \leqslant N, \qquad u_i^{(1)} = u_i, \qquad x_i(0) = x_i^0, \tag{1.2}$$

and

$$y = f(x) = \frac{1}{2}\big(|x+1| - |x-1|\big) \tag{1.3}$$

is the output function. For $1 \leqslant n \leqslant N$, parameter $A^{(n)} = (a_{-d}^{(n)}, \ldots, a_d^{(n)})$ is called the feedback template; $B^{(n)} = (b_{-d}^{(n)}, \ldots, b_d^{(n)})$ is called the controlling template, and $z^{(n)}$ is the threshold. The quantity $x_i^{(n)}$ denotes the state of a cell C_i in the nth layer. The stationary solutions $\bar{x} = (\bar{x}_i^{(n)})$ of (1.1) are essential for understanding the system, and their outputs $\bar{y}_i^{(n)} = f(\bar{x}_i^{(n)})$ are called patterns. A mosaic solution $(\bar{x}_i^{(n)})$ satisfies $|\bar{x}_i^{(n)}| > 1$ for all i, n. Hence the investigation of stationary solution of N-layer CNN is to study an N-coupled map lattice,

$$\begin{cases} x_i^{(1)} = \displaystyle\sum_{|k|\leqslant d} a_k^{(1)} y_{i+k}^{(1)} + \sum_{|k|\leqslant d} b_k^{(1)} u_{i+k}^{(1)} + z^{(1)}, \\ x_i^{(2)} = \displaystyle\sum_{|k|\leqslant d} a_k^{(2)} y_{i+k}^{(2)} + \sum_{|k|\leqslant d} b_k^{(2)} y_{i+k}^{(1)} + z^{(2)}, \\ \quad \vdots \\ x_i^{(N)} = \displaystyle\sum_{|k|\leqslant d} a_k^{(N)} y_{i+k}^{(N)} + \sum_{|k|\leqslant d} b_k^{(N)} y_{i+k}^{(N-1)} + z^{(N)}. \end{cases} \tag{1.4}$$

One-layer CNN with input is first considered. Let

$$\mathcal{P}^{n+2} = \big\{(A, B, z)\colon\ A, B \in \mathcal{M}_{1\times(2d+1)}(\mathbb{R}),\ z \in \mathbb{R}\big\}, \tag{1.5}$$

where $n = 4d + 1$. The parameter space $\mathcal{P}^{n+2}$ can be partitioned into finite subregions, such that each region has the same mosaic patterns. Once the region of the parameter space is chosen, the basic set of admissible local patterns $\mathcal{B} \subseteq \{+, -\}^{\mathbb{Z}_{3\times 2}}$ is then determined. The ordering matrix of all local patterns in $\{+, -\}^{\mathbb{Z}_{3\times 2}}$ is defined. For a given basic set $\mathcal{B}$, the transition matrix $\mathbf{T}(\mathcal{B})$ is then obtained, and a shift space is induced. For simplicity, consider the case $d = 1$, i.e., each cell can only interact with their nearest neighbors. In one-dimensional one-layer CNN without input,

every partition is associated with a unique set of admissible patterns $\overline{\mathcal{B}} = \mathcal{B}_{3\times 1}$ and the transition matrix $\overline{\mathbf{T}} = \mathbf{T}(\mathcal{B}_{3\times 1})$ [15]. Let

$$Y = \left\{ (y_i)_{i\in\mathbb{Z}} \;\middle|\; y_{i-1}y_iy_{i+1} \in \overline{\mathcal{B}} \text{ for all } i \in \mathbb{Z} \right\}, \tag{1.6}$$

then Y is a shift of finite type (SOFT). The number of global admissible patterns with length n and the number of periodic patterns with period m can then be formulated from the transition matrix $\overline{\mathbf{T}}$. However, this cannot be done when the basic set of admissible local patterns $\mathcal{B} = \mathcal{B}_{3\times 2}$ is derived from the one-layer CNN with input. More precisely, each pattern that is produced from the system is a coupled pattern $\begin{smallmatrix} y_1y_2y_3 \\ u_1u_2u_3 \end{smallmatrix}$, where $y_1y_2y_3$ denotes the output pattern, and $u_1u_2u_3$ denotes the input pattern. For simplicity, rewrite the coupled pattern as $y_1y_2y_3 \diamond u_1u_2u_3$. The output space is defined as

$$Y_U = \left\{ \begin{array}{l} (\cdots y_{-1}y_0y_1\cdots) \in \{+,-\}^{\mathbb{Z}}\text{: there exists } (\cdots u_{-1}u_0u_1\cdots) \in \{+,-\}^{\mathbb{Z}} \\ \quad \text{such that } (\cdots y_{-1}y_0y_1\cdots\diamond\cdots u_{-1}u_0u_1\cdots) \in \Sigma(\mathcal{B}) \end{array} \right\}, \tag{1.7}$$

where $\Sigma(\mathcal{B}) \subseteq \{+,-\}^{\mathbb{Z}_{\infty\times 2}}$ is a subshift space generated by $\mathcal{B} \subseteq \{+,-\}^{\mathbb{Z}_{3\times 2}}$. Analytical results indicate that Y_U is not a SOFT, but a sofic shift (Theorem 2.13). Under this situation, the formula of spatial entropy (entropy) $h(\mathcal{B})$ (Theorem 2.17) and dynamical zeta function (zeta function) $\zeta_\sigma(t)$ (Theorem 2.24) can be computed. Therefore, the dynamics of the mosaic solutions of multi-layer CNN are understood. Conversely, the sofic shift is realized through a realistic model.

The analysis gets more complicated in N-layer CNN, $N \geqslant 2$. However, once recognizing the elaborate content of one-layer CNN with input, all results for one-layer CNN with input can be extended to general case with analogous method. We like to emphasize that each layer induces a sofic shift and the N-layer coupled system induces the convolution of N-many independent sofic shifts. Hence, Section 2 studies one-layer CNN with and without input and emphases the difference. Without input, the dynamical system is subshift of finite type and then sofic when input appears. Section 3 consists those general results introduced in Section 2.

The dynamics of multi-layer CNN with input produce a phenomenon that is never seen in one-layer CNN without input. The entropy of the one-layer CNN without input has a "symmetry" about the parameters. More precisely, consider the one-dimensional CNN,

$$\frac{dx_i}{dt} = -x_i + a_l y_{i-1} + a y_i + a_r y_{i+1} + z, \tag{1.8}$$

and select one of the partitions of parameter space $\{(a_l, a_r)\text{: } a_l, a_r \in \mathbb{R}\} = \mathbb{R}^2$. The parameters a and z thus have 25 subregions, each with the same entropy. Furthermore,

$$h\big(\mathcal{B}\big([m,n]\big)\big) = h\big(\mathcal{B}\big([n,m]\big)\big) \quad \text{for } 0 \leqslant m, n \leqslant 4. \tag{1.9}$$

The details as in [15]. However, when considering multi-layer CNN with input, not only the entropy and zeta function are varied, but the symmetry of the entropy is broken even for the simplest case one-layer CNN with input. Hence, input adding for a CNN system is the main mechanism that breaks the symmetry of entropy.

The rest of this study is organized as follows. Section 2 describes the complexity of the global set of output patterns for one-layer CNN with input. The entropy and zeta function can be exactly computed through the induced sofic shift space. Section 3 extends all results in Section 2 to N-layer CNN, where $N \geqslant 2$. Finally, Appendix A lists the detail of the partition in Example 2.5.

2. One-layer cellular neural networks with input

The complexity of the global set of output patterns for one-layer CNN with input is investigated in this section.

2.1. Ordering matrix and transition matrix

In this section, the parameter space $\mathcal{P}^{n+2}$ as in (1.5) will be partitioned into finite subregions, such that each region has the same mosaic patterns. Once the region of the parameter space is chosen, the basic set of admissible local patterns $\mathcal{B} \subseteq \{+,-\}^{\mathbb{Z}_{3\times 2}}$ is then determined. Then, the ordering matrix of all local patterns in $\{+,-\}^{\mathbb{Z}_{3\times 2}}$ will be defined. For a given basic set $\mathcal{B}$, the transition matrix $\mathbf{T}(\mathcal{B})$ will be obtained.

2.1.1. Partition of parameter space

This subsection explores the relationship between the parameters of templates and the admissible local output patterns. The differential equation of CNN with input is of the form

$$\frac{dx_i}{dt} = -x_i + \sum_{|k|\leqslant d} a_k y_{i+k} + \sum_{|\ell|\leqslant d} b_\ell u_{i+\ell} + z, \tag{2.1}$$

where $A = [-a_d, \ldots, a, \ldots, a_d]$, $B = [-b_d, \ldots, b, \ldots, b_d]$ are the feedback and controlling templates, respectively, $y = f(x) = \frac{1}{2}(|x+1| - |x-1|)$ is the output function, z is the threshold, and $a \equiv a_0, b \equiv b_0$.

The quantity x_i represents the state of the cell at i. The stationary solution $\bar{x} = (\bar{x}_i)$ of (2.1) satisfies

$$\bar{x}_i = \sum_{|k|\leqslant d} a_k \bar{y}_{i+k} + \sum_{|\ell|\leqslant d} b_\ell u_{i+\ell} + z.$$

The output $\bar{y} = (\bar{y}_i)$ is called output pattern. A mosaic solution $\bar{x}$ satisfies $|\bar{x}_i| > 1$ and its corresponding pattern $\bar{y}$ is called a mosaic output pattern. Consider the mosaic solution $\bar{x}$, the necessary and sufficient conditions for state "+" at cell C_i, i.e., $\bar{x}_i > 1$, are

$$a - 1 + z > -\Bigg(\sum_{0<|k|\leqslant d} a_k \bar{y}_{i+k} + \sum_{|\ell|\leqslant d} b_\ell u_{i+\ell} \Bigg). \tag{2.2}$$

Similarly, the necessary and sufficient conditions for state "−" at cell C_i, i.e., $\bar{x}_i < -1$, are

$$a - 1 - z > \sum_{0<|k|\leqslant d} a_k \bar{y}_{i+k} + \sum_{|\ell|\leqslant d} b_\ell u_{i+\ell}. \tag{2.3}$$

For simplicity, denote $\bar{y}_i$ by y_i and rewrite the output patterns $y_{-d} \cdots y \cdots y_d$ coupled with input $u_{-d} \cdots u \cdots u_d$ as

$$\begin{matrix} y_{-d} \cdots y \cdots y_d \\ u_{-d} \cdots u \cdots u_d \end{matrix} = Y \diamond U, \tag{2.4}$$

where $Y = y_{-d} \cdots y \cdots y_d$, $U = u_{-d} \cdots u \cdots u_d$. Let

$$V^n = \{v \in \mathbb{R}^n\colon\ v = (v_1, v_2, \ldots, v_n),\ \text{and } |v_i| = 1,\ 1 \leqslant i \leqslant n\},$$

where $n = 4d+1$, (2.2) and (2.3) can be rewritten in a compact form by introducing the following notation.

Denote $\alpha = (a_{-d}, \ldots, a_{-1}, a_1, \ldots, a_d)$, $\beta = (b_{-d}, \ldots, b, \ldots, b_d)$. Then, α can be used to represent A', the surrounding template of A without center, and β can be used to represent the template B. The basic set of admissible local patterns with "+" state in the center is defined as

$$\mathcal{B}(+, A, B, z) = \{v \diamond w \in V^n\colon\ a - 1 + z > -(\alpha \cdot v + \beta \cdot w)\}, \tag{2.5}$$

where $\cdot$ is the inner product in Euclidean space. Similarly, the basic set of admissible local patterns with "−" state in the center is defined as

$$\mathcal{B}(-, A, B, z) = \{v' \diamond w' \in V^n\colon\ a - 1 - z > \alpha \cdot v + \beta \cdot w\}. \tag{2.6}$$

Furthermore, the admissible local patterns induced by (A, B, z) can be denoted by

$$\mathcal{B}(A, B, z) = \big(\mathcal{B}(+, A, B, z), \mathcal{B}(-, A, B, z)\big). \tag{2.7}$$

Let

$$\mathcal{P}^{n+2} = \{(A, B, z) \mid A, B \in \mathcal{M}_{1\times(2d+1)}(\mathbb{R}),\ z \in \mathbb{R}\}, \tag{2.8}$$

where $\mathcal{M}_{r\times s}(\mathbb{R})$ means an $r \times s$ real matrix. $\mathcal{P}^{n+2}$ can be partitioned so that each subregion generates the same mosaic patterns, when the controlling template $B \equiv 0$ is proved in [14]. The general results for $B \neq 0$ can be obtained similarly, so the detailed proof is omitted for simplicity.

Theorem 2.1. *There exists positive integer $K(n)$ and a unique collection of open subsets $\{P_k\}_{k=1}^K$ of $\mathcal{P}^{n+2}$ satisfying*

(i) $\mathcal{P}^{n+2} = \bigcup_{k=1}^K \overline{P}_k$;
(ii) $P_k \cap P_\ell = \emptyset$ *for all* $k \neq \ell$;
(iii) $\mathcal{B}(A, B, z) = \mathcal{B}(\tilde{A}, \tilde{B}, \tilde{z})$ *if and only if* $(A, B, z), (\tilde{A}, \tilde{B}, \tilde{z}) \in P_k$ *for some* k.

Here $\overline{P}$ is the closure of P in $\mathcal{P}^{n+2}$.

2.1.2. Ordering matrix

This subsection defines the ordering matrix $\mathbb{X} = \mathbb{X}_{3\times 2}$ of all possible local patterns in $\{+, -\}^{\mathbb{Z}_{3\times 2}}$. First, the notation of the pattern with size 3×1 is considered.

Let

$$a_{00} = --, \qquad a_{01} = -+, \qquad a_{10} = +-, \qquad a_{11} = ++, \tag{2.9}$$

defining

$$a_{i_1 i_2} a_{i_2' i_3} = \emptyset \quad \Leftrightarrow \quad i_2 \neq i_2'. \tag{2.10}$$

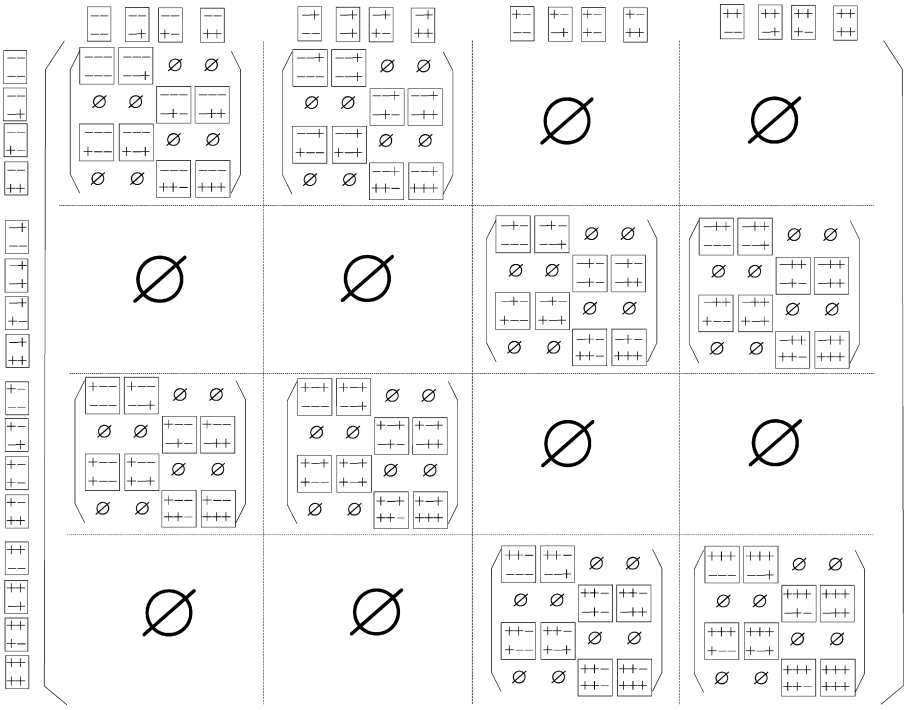

Fig. 2.1. The ordering matrix of all local patterns in $\mathbb{Z}_{3\times 2}$.

If $a_{i_1 i_2} a_{i'_2 i_3} \neq \emptyset$, then denote it by $a_{i_1} a_{i_2} a_{i_3}$ and it is a pattern with size 3×1. Define

$$\mathbb{X} = \begin{bmatrix} X_{11} & X_{12} & X_{13} & X_{14} \\ X_{21} & X_{22} & X_{23} & X_{24} \\ X_{31} & X_{32} & X_{33} & X_{34} \\ X_{41} & X_{42} & X_{43} & X_{44} \end{bmatrix}, \qquad X_{ij} = \begin{bmatrix} x_{ij;11} & x_{ij;12} & x_{ij;13} & x_{ij;14} \\ x_{ij;21} & x_{ij;22} & x_{ij;23} & x_{ij;24} \\ x_{ij;31} & x_{ij;32} & x_{ij;33} & x_{ij;34} \\ x_{ij;41} & x_{ij;42} & x_{ij;43} & x_{ij;44} \end{bmatrix} \tag{2.11}$$

for $1 \leqslant i, j \leqslant 4$ as in Fig. 2.1. $x_{ij;kl}$ means the pattern $\begin{smallmatrix} a_{r_1 r_2} a_{r'_2 r_3} \\ a_{s_1 s_2} a_{s'_2 s_3} \end{smallmatrix}$, where

$$\begin{aligned} r_1 &= \left[\frac{i-1}{2}\right], \qquad r_2 = i - 1 - 2r_1, \qquad r'_2 = \left[\frac{j-1}{2}\right], \qquad r_3 = j - 1 - 2r'_2, \\ s_1 &= \left[\frac{k-1}{2}\right], \qquad s_2 = k - 1 - 2s_1, \qquad s'_2 = \left[\frac{l-1}{2}\right], \qquad s_3 = l - 1 - 2s'_2, \end{aligned} \tag{2.12}$$

and $[\cdot]$ is the Gauss function.

If $a_{r_1 r_2} a_{r'_2 r_3} = \emptyset$ or $a_{s_1 s_2} a_{s'_2 s_3} = \emptyset$, then $x_{ij;kl} = \emptyset$. Furthermore, if $x_{ij;kl} \neq \emptyset$, then it is denoted by the pattern $\begin{smallmatrix} a_{r_1} a_{r_2} a_{r_3} \\ a_{s_1} a_{s_2} a_{s_3} \end{smallmatrix}$ in $\{+, -\}^{\mathbb{Z}_{3\times 2}}$. Hence, the self-similar property appear in $\mathbb{X}$ as in Fig. 2.1, i.e., the upper pattern of X_{ij} is the same as the lower pattern of $x_{kl;ij}$, for $1 \leqslant i, j, k, l \leqslant 4$. Once

the basic set of admissible local patterns $\mathcal{B} \subseteq \{+,-\}^{\mathbb{Z}_{3\times 2}}$ is given, define $\Sigma_{n\times 2}(\mathcal{B})$ the collection of all patterns with size $n \times 2$ generated by $\mathcal{B}$ as

$$\Sigma_{n\times 2}(\mathcal{B}) = \left\{ \begin{matrix} y_1 y_2 \cdots y_n \\ u_1 u_2 \cdots u_n \end{matrix} \in \{+,-\}^{\mathbb{Z}_{n\times 2}} : \begin{matrix} y_{i-1} y_i y_{i+1} \\ u_{i-1} u_i u_{i+1} \end{matrix} \in \mathcal{B} \text{ for all } 2 \leqslant i \leqslant n-1 \right\}. \quad (2.13)$$

For simplicity, rewrite $\begin{matrix} y_1 y_2 \cdots y_n \\ u_1 u_2 \cdots u_n \end{matrix}$ as $y_1 y_2 \cdots y_n \diamond u_1 u_2 \cdots u_n$, where $y_i, u_i \in \{+,-\}$, $1 \leqslant i \leqslant n$.

To measure the complexity of the global set of output patterns, the following subshift space in $\{+,-\}^{\mathbb{Z}}$ is considered. Define the output space $Y_U \equiv Y_U(\mathcal{B})$ by

$$Y_U = \left\{ \begin{matrix} (\cdots y_{-1} y_0 y_1 \cdots) \in \{+,-\}^{\mathbb{Z}} : \text{ there exists } (\cdots u_{-1} u_0 u_1 \cdots) \in \{+,-\}^{\mathbb{Z}} \\ \text{such that } (\cdots y_{-1} y_0 y_1 \cdots \diamond \cdots u_{-1} u_0 u_1 \cdots) \in \Sigma(\mathcal{B}) \end{matrix} \right\}, \quad (2.14)$$

where $\Sigma(\mathcal{B}) \subseteq \{+,-\}^{\mathbb{Z}_{\infty\times 2}}$ is a subshift space generated by $\mathcal{B} \subseteq \{+,-\}^{\mathbb{Z}_{3\times 2}}$.

2.1.3. Transition matrix

This subsection derives the transition matrix for a given basic set $\mathcal{B}$. The transition matrix $\mathbf{T}$ is defined as

$$\mathbf{T}(\mathcal{B}) = (T_{ij}), \quad 1 \leqslant i, j \leqslant 4, \quad (2.15)$$

where $T_{ij} = (t_{ij;kl}) \in \mathcal{M}_{4\times 4}(\mathbb{R})$ and

$$t_{ij;kl} = \begin{cases} 1, & \text{if } x_{ij;kl} \in \mathcal{B}, \\ 0, & \text{if } x_{ij;kl} \in \{+,-\}^{\mathbb{Z}_{3\times 2}} \setminus \mathcal{B} \text{ or } x_{ij;kl} = \emptyset, \end{cases} \quad (2.16)$$

where $x_{ij;kl} = \begin{matrix} a_{r_1 r_2} a_{r'_2 r_3} \\ a_{s_1 s_2} a_{s'_2 s_3} \end{matrix}$ satisfies (2.12). Once $\mathbf{T}(\mathcal{B})$ is constructed, it is then rewritten as $\mathbf{T}(\mathcal{B}) = (t_{pq}) \in \mathcal{M}_{16\times 16}(\mathbb{R})$, where

$$t_{pq} = t_{ij;kl} \quad \text{for } p = 4(i-1)+k,\ q = 4(j-1)+l. \quad (2.17)$$

If templates A, B and threshold z are given, then the basic set $\mathcal{B}(A, B, z)$ is obtained from Theorem 2.1. Moreover, the transition matrix $\mathbf{T}$ is immediately derived from (2.16) and (2.17).

If a set of input patterns $\mathcal{U} \equiv \{u_1 u_2 u_3\} \subseteq \{+,-\}^{\mathbb{Z}_{3\times 1}}$ is assigned, then the basic set of admissible local patterns is denoted by

$$\mathcal{B}\big((A, B, z); \mathcal{U}\big) = \left\{ \begin{matrix} y_1 y_2 y_3 \\ u_1 u_2 u_3 \end{matrix} \in \mathcal{B}(A, B, z) : u_1 u_2 u_3 \in \mathcal{U} \right\}. \quad (2.18)$$

The transition matrix for $\mathcal{U}$ is defined by $\mathbf{U} = (u_{ij}) \in \mathcal{M}_{4\times 4}(\mathbb{R})$, where

$$u_{ij} = \begin{cases} 1, & \text{if } u_1 u_2 u_3 \in \mathcal{U}, \\ 0, & \text{otherwise.} \end{cases} \quad (2.19)$$

If $\hat{\mathbf{T}}$ denotes the transition matrix of $\mathcal{B}((A, B, z); \mathcal{U})$, then the following theorem is obtained. Before the theorem is stated, two products of matrices are defined as follows.

Definition 2.2. For any two matrices $\mathbf{M} = (m_{ij}) \in \mathcal{M}_{k\times k}(\mathbb{R})$, $\mathbf{N} = (n_{i'j'}) \in \mathcal{M}_{\ell\times\ell}(\mathbb{R})$, the Kronecker product (tensor product) $\mathbf{M}\otimes\mathbf{N}$ of $\mathbf{M}$ and $\mathbf{N}$ is defined by

$$\mathbf{M}\otimes\mathbf{N} = (m_{ij}\mathbf{N}) \in \mathcal{M}_{k\ell\times k\ell}(\mathbb{R}). \tag{2.20}$$

Next, for any $\mathbf{P} = (p_{ij}), \mathbf{Q} = (q_{ij}) \in \mathcal{M}_{r\times r}(\mathbb{R})$, the Hadamard product $\mathbf{P}\circ\mathbf{Q}$ of $\mathbf{P}$ and $\mathbf{Q}$ is defined by

$$\mathbf{P}\circ\mathbf{Q} = (p_{ij}q_{ij}) \in \mathcal{M}_{r\times r}(\mathbb{R}). \tag{2.21}$$

Theorem 2.3. *If (A, B, z) and $\mathcal{U}$ are given, then*

$$\hat{\mathbf{T}}\big(\mathcal{B}\big((A, B, z); \mathcal{U}\big)\big) = \mathbf{T}\big(\mathcal{B}(A, B, z)\big)\circ(E_4\otimes\mathbf{U}), \tag{2.22}$$

where $\circ$ and $\otimes$ is the Hadamard product and Kronecker product in Definition 2.2*, respectively, $E_4 = (e_{ij}) \in \mathcal{M}_{4\times4}(\mathbb{R})$ with $e_{ij} = 1$ for all i, j, is the full matrix.*

Proof. Let the transition matrix $\hat{\mathbf{T}} = (\hat{t}_{pq}) \in \mathcal{M}_{16\times16}(\mathbb{R})$, rewriting $\hat{t}_{pq} = \hat{t}_{ij;kl}$, where

$$i = \left[\frac{p-1}{4}\right] + 1, \qquad j = p - 4(i-1), \qquad k = \left[\frac{q-1}{4}\right] + 1,$$

and $l = q - 4(j-1)$. By (2.16) and (2.18), $\hat{t}_{pq} = \hat{t}_{ij;kl} = t_{ij;kl}\cdot u_{kl}$ is obtained. This completes the proof. □

2.1.4. Patterns generation

This subsection introduces the patterns generation problem induced by (A, B, z). Some results of patterns generation problem induced by (A, z) must be recalled before stating the main theory [18]. The basic set of admissible local patterns $\mathcal{B}(A, z) \equiv \mathcal{B}$ is then determined once (A, z) is given. The shift space generated by $\mathcal{B}$, denoted by $\Sigma(\mathcal{B})$, is given by

$$\Sigma(\mathcal{B}) = \big\{y = (y_i)_{i\in\mathbb{Z}} \in \{+,-\}^{\mathbb{Z}}\colon\ y_{i-1}y_iy_{i+1} \in \mathcal{B} \text{ for all } i \in \mathbb{Z}\big\}. \tag{2.23}$$

The shift space $\Sigma(\mathcal{B})$ is thus a subshift of finite type for all $\mathcal{B} = \mathcal{B}(A, z)$. Let $\Sigma_n(\mathcal{B})$ denote the set of n-blocks (i.e., the pattern with size $n\times1$) in $\Sigma(\mathcal{B})$, and $\Gamma_n(\mathcal{B})$ denote the number of the set of n-blocks. The theorem follows below [18].

Theorem 2.4. *If $\mathcal{B} = \mathcal{B}(A, z)$ is given, $\mathbf{T}$ is the transition matrix induced by $\mathcal{B}$, then $\Gamma_n(\mathcal{B}) = |\mathbf{T}^{n-2}|$ for all $n \in \mathbb{N}$, $n \geqslant 3$, where $|\mathbf{T}| \equiv \sum_{1\leqslant i,j\leqslant k}|t_{ij}|$ for all $\mathbf{T} = (t_{ij}) \in \mathcal{M}_{k\times k}(\mathbb{R})$.*

Consider (A, B, z) with $B \neq 0$, let $\mathcal{B}(A, B, z) \equiv \mathcal{B}$ denote the basic set of admissible local patterns, $\Sigma_n(Y_U)$ denote the set of n-blocks in Y_U, i.e.,

$$\Sigma_n(Y_U) = \left\{ \begin{array}{l} y = (y_i)_{i=1}^n \in \{+,-\}^{\mathbb{Z}_{n\times1}}\colon \exists u = (u_i)_{i=1}^n \in \{+,-\}^{\mathbb{Z}_{n\times1}} \\ \quad \text{such that } y\diamond u \in \Sigma_n(\mathcal{B}) \end{array} \right\}, \tag{2.24}$$

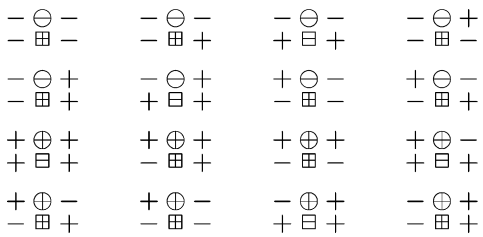

Fig. 2.2. The basic set of patterns for some templates A, B, z and input $\mathcal{U}$.

and $\Gamma_n(Y_U)$ denote the number of n-blocks of output patterns generated by $\mathcal{B}$. Theorem 2.4 is invalid in general for deriving the precise value of $\Gamma_n(Y_U)$ for $n \in \mathbb{N}$. An example is given below. Appendix A explains the theorem in detail.

Example 2.5. Let $A = [a_l, a, a_r]$, $B = [b_l, b, b_r]$ satisfy the following conditions:

(i) $a_l > b_l > a_r > b > b_r > 0$.
(ii) $a_l + b > a_r + b_l + b_r$, $a_l + b_r > b_l + b$.
(iii) $b_l + b > a_l > a_r + b + b_r$.
(iv) $a_r + b > b_l + b_r$, $b_l > a_r + b_r$, $a_r > b + b_r$.

The positions of ℓ_i^+ and ℓ_j^- on the $(a-1, z)$ plane are determined exactly as in Appendix A. Given region $R = [23, 18]$, i.e., R is bounded by ℓ_{23}^+, ℓ_{24}^+, ℓ_{18}^- and ℓ_{19}^-, and the set of input patterns is given by $\mathcal{U} = \{-+-, -++, +-+\}$. Thus, Fig. 2.2 illustrates the basic set of admissible local patterns $\mathcal{B} = \mathcal{B}((A, B, z); \mathcal{U})$.

According to Theorem 2.3, the transition matrix of $\mathcal{B}((A, B, z); \mathcal{U})$ is

$$\hat{\mathbf{T}} = \hat{\mathbf{T}}\big(\mathcal{B}\big((A, B, z); \mathcal{U}\big)\big) = \begin{pmatrix} \hat{T}_{11} & \hat{T}_{12} & 0 & 0 \\ 0 & 0 & 0 & \hat{T}_{24} \\ \hat{T}_{31} & 0 & 0 & 0 \\ 0 & 0 & \hat{T}_{43} & \hat{T}_{44} \end{pmatrix},$$

where

$$\hat{T}_{11} = \hat{T}_{12} = \hat{T}_{43} = \hat{T}_{44} = \begin{pmatrix} 0 & 0 & 0 & 0 \\ 0 & 0 & 1 & 1 \\ 0 & 1 & 0 & 0 \\ 0 & 0 & 0 & 0 \end{pmatrix}, \qquad \hat{T}_{31} = \begin{pmatrix} 0 & 0 & 0 & 0 \\ 0 & 0 & 1 & 1 \\ 0 & 0 & 0 & 0 \\ 0 & 0 & 0 & 0 \end{pmatrix},$$

$$\hat{T}_{24} = \begin{pmatrix} 0 & 0 & 0 & 0 \\ 0 & 0 & 0 & 1 \\ 0 & 1 & 0 & 0 \\ 0 & 0 & 0 & 0 \end{pmatrix}.$$

From the transition matrix, the output patterns $\{-++, ++-, +--\}$ exist. By the concept of subshift of finite type, the output pattern $-++--$ is admissible. However, there exists no $u_1u_2u_3u_4u_5 \in \Sigma_5(\mathcal{U})$ such that $-++--\diamond u_1u_2u_3u_4u_5 \in \Sigma_5(\mathcal{B})$. This finding shows that the inner structure needs to be considered. More precisely, since $\hat{T}_{24}\hat{T}_{43}\hat{T}_{31} = 0$, no input could possibly produce the output pattern $-++--$.

So far, this work has shown that $\Gamma_n(Y_U) \neq |\hat{\mathbf{T}}^{n-2}|$ in general, since different input patterns might have the same output pattern. To overcome this difficulty, the next subsection introduces the concept of sofic shift in the symbolic dynamical system.

2.2. Definition and background of sofic shifts

This subsection recalls some definitions and main results of sofic shifts. Lind and Marcus has described sofic shifts in detail [18].

Definition 2.6. A labeled graph $\mathcal{G} = (G, \mathcal{L})$ consists of an underlying graph G with edge set $\mathcal{E}$, and the labeling $\mathcal{L} : \mathcal{E} \to \mathcal{A}$ assigns to each edge a label from the finite alphabet $\mathcal{A}$. A sofic shift is defined by $\mathbf{X} = \mathbf{X}_{\mathcal{G}}$ for some labeled graph $\mathcal{G}$.

Definition 2.7. A labeled graph $\mathcal{G} = (G, \mathcal{L})$ is right-resolving if, for each vertex of I of G, the edges starting from I carry different labels. In other words, $\mathcal{G}$ is right-resolving if, for each I, the restriction of $\mathcal{L}$ to $\mathcal{E}_I$ is one-to-one, where $\mathcal{E}_I$ consists of those edges starting from I.

The following theorem shows that every sofic shift has a right-resolving presentation. The method for finding an explicit right-resolving presentation is called the subset construction method.

Subset construction method. Let $\mathbf{X}$ be a sofic shift over the alphabet $\mathcal{A}$ having a presentation $\mathcal{G} = (G, \mathcal{L})$ so that $\mathbf{X} = \mathbf{X}_{\mathcal{G}}$. If $\mathcal{G}$ is not right-resolving, then a new labeled graph $\mathcal{H} = (H, \mathcal{L}')$ is constructed as follows.

The vertices I of H are the nonempty subsets of the vertex set $\mathcal{V}(G)$ of G. If $I \in \mathcal{V}(H)$ and $a \in \mathcal{A}$, let J denote the set of terminal vertices of edges in G starting at some vertices in I and labeled a, i.e., J is the set of vertices reachable from I using the edges labeled a. There are two cases.

1. If $J = \emptyset$, do nothing.
2. If $J \neq \emptyset$, $J \in \mathcal{V}(H)$ and draw an edge in H from I to J labeled a.

Carrying this out for each $I \in \mathcal{V}(H)$ and each $a \in \mathcal{A}$ produces the labeled graph $\mathcal{H}$. Then, each vertex I in H has at most one edge with a given label starting at I. This implies that $\mathcal{H}$ is right-resolving.

Theorem 2.8. *Let $\mathcal{G} = (G, \mathcal{L})$ be a labeled graph which is not right-resolving, $\mathcal{H} = (H, \mathcal{L}')$ be a right-resolving labeled graph constructed under the subset construction method. Then $\mathbf{X}_{\mathcal{G}} = \mathbf{X}_{\mathcal{H}}$, i.e., $\mathcal{G}$ and $\mathcal{H}$ present the same shift space.*

2.3. Entropy and zeta function

This subsection investigates the entropy and zeta function for the global set of output patterns using the concepts of sofic shifts.

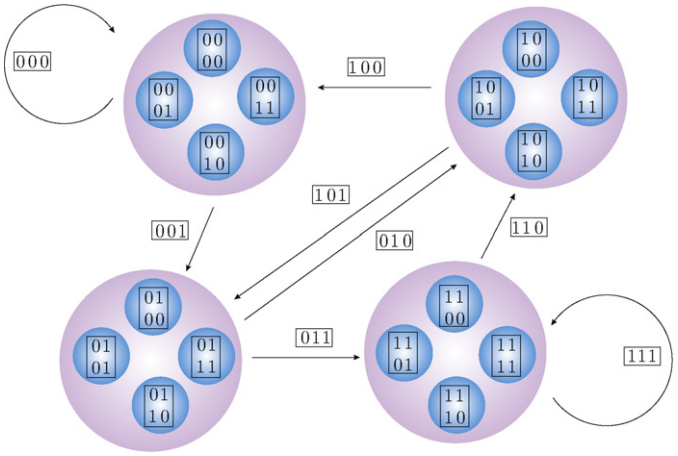

Fig. 2.3. The labeled graph of CNN with input.

2.3.1. Sofic shift

This subsection shows that the output space of one-layer CNN with input is a sofic shift. For a given basic set $\mathcal{B}$, the transition matrix $\mathbf{T}$ is defined as (2.15)–(2.17). Let the alphabet $\mathcal{S} = \{s_{ij}\}_{1\leqslant i,j\leqslant 4}$, where

$$s_{ij} = a_{r_1 r_2} a_{r'_2 r_3}, \tag{2.25}$$

$a_{r_k r_{k+1}}$ is defined in (2.9), and

$$r_1 = \left[\frac{i-1}{2}\right], \qquad r_2 = i - 1 - 2r_1, \qquad r'_2 = \left[\frac{j-1}{2}\right], \qquad r_3 = j - 1 - 2r'_2. \tag{2.26}$$

By (2.10), $s_{ij} = \emptyset$ if $r_2 \neq r'_2$. The symbolic transition matrix is defined as

$$\mathbf{S} = (s_{ij} T_{ij})_{1\leqslant i,j\leqslant 4} = (s_{ij} t_{ij;kl}) \in \mathcal{M}_{16\times 16}(\mathbb{R}), \tag{2.27}$$

where $s_{ij} t_{ij;kl} = \emptyset$ if $s_{ij} = \emptyset$ or $t_{ij;kl} = 0$. Rewrite $\mathbf{S} = (\tilde{s}_{pq})$, where $\tilde{s}_{pq} = s_{ij} t_{ij;kl}$ for

$$p = 4(i-1) + k, \qquad q = 4(j-1) + l.$$

Let $G_{\mathbf{T}}$ be the underlying graph induced by $\mathbf{T}$ with edge set

$$\mathcal{E} = \{e_{pq} \colon t_{pq} = 1,\ 1 \leqslant p, q \leqslant 16\},$$

and the labeling $\mathcal{L} : \mathcal{E} \to \mathcal{S}$ defined by $\mathcal{L}(e_{pq}) = s_{ij}$. $\mathcal{G}_{\mathbf{S}} = (G_{\mathbf{T}}, \mathcal{L})$ is thus a labeled graph as in Fig. 2.3. By (2.25), a word $s_{i_1 i_2} s_{i_2 i_3}$ in $\mathcal{S}^{\mathbb{Z}}$ can be defined by $s_{i_1 i_2} s_{i_2 i_3} = a_{r_1 r_2} a_{r_2 r_3} a_{r_3 r_4}$. The edge

shift with alphabet $\mathcal{S}$ is defined by

$$\mathbf{X}_{\mathcal{G}_\mathbf{S}} = \left\{ \begin{array}{l} (\cdots s_{i_{-1}i_0} s_{i_0 i_1} s_{i_1 i_2} \cdots) \in \mathcal{S}^{\mathbb{Z}}\text{: there exists } (\cdots k_{-1}k_0k_1\cdots) \\ \quad \text{such that } t_{i_j i_{j+1};k_j k_{j+1}} \neq 0 \text{ for all } j \in \mathbb{Z} \end{array} \right\}. \tag{2.28}$$

The following theorem is thus obtained.

Theorem 2.9. $\mathbf{X} = \mathbf{X}_{\mathcal{G}_\mathbf{S}}$ *is a sofic shift.*

The relationship between output space Y_U and induced sofic shift $\mathbf{X}_{\mathcal{G}_\mathbf{S}}$ is then investigated.

Definition 2.10. Let $\mathcal{A}$, $\mathcal{U}$ be finite alphabets, $\mathbf{X}$ be a shift space over $\mathcal{A}$, $B_k(\mathbf{X})$ denote the set of k-blocks that occur in points in $\mathbf{X}$, $\Phi : B_{m+n+1}(\mathbf{X}) \to \mathcal{U}$ be a block map. Then the map $\phi : \mathbf{X} \to \mathcal{U}^{\mathbb{Z}}$ defined by $y = \phi(x)$ with

$$y_i = \Phi(x_{i-m} \cdots x_{i-1} x_i x_{i+1} \cdots x_{i+n}) = \Phi(x_{[i-m,i+n]})$$

is called the sliding block code with memory m and anticipate n induced by Φ.

Let $\Sigma_3(Y_U)$ be the set of 3-blocks in Y_U as in (2.24). A block map $\Phi : \Sigma_3(Y_U) \to \mathcal{S}$ is thus defined by

$$\Phi(y_i y_{i+1} y_{i+2}) = s_{\Psi(y_i y_{i+1})\Psi(y_{i+1} y_{i+2})}, \tag{2.29}$$

where $\Psi(y_i y_{i+1}) = 1 + \varphi(y_{i+1}) + 2\varphi(y_i)$ and φ is defined by $\varphi(+) = 1$ and $\varphi(-) = 0$. Then the map $\phi : Y_U \to \mathcal{S}^{\mathbb{Z}}$ defined by

$$\phi(\cdots y_{-1} y_0 y_1 \cdots) = (\cdots s_{i_{-1}i_0} s_{i_0 i_1} s_{i_1 i_2} \cdots) \tag{2.30}$$

with $s_{i_k i_{k+1}} = \Phi(y_{i_k} y_{i_{k+1}} y_{i_{k+2}})$ is a sliding block code from Y_U to $\mathbf{X}_{\mathcal{G}_\mathbf{S}}$.

Definition 2.11. Let $\phi : \mathbf{X} \to \mathbf{Y}$ be a sliding block code, then ϕ is a conjugacy if ϕ is invertible. It is also called $\mathbf{X}$ is conjugate to $\mathbf{Y}$.

Theorem 2.12. *(See [18].) If a sliding code is one-to-one and onto, then it is a conjugacy.*

The conjugacy between Y_U and $\mathbf{X}_{\mathcal{G}_\mathbf{S}}$ can be proved now.

Theorem 2.13. *Given a basic set $\mathcal{B}$, the transition matrix* $\mathbf{T}$ *and the output space Y_U are then obtained. Let $\mathcal{G}_\mathbf{S} = (G_\mathbf{T}, \mathcal{L})$ be the labeled graph induced by $\mathcal{B}$, then Y_U is conjugate to $\mathbf{X}_{\mathcal{G}_\mathbf{S}}$ under the sliding block code ϕ defined in* (2.30)*.*

Proof. It suffices to prove that ϕ is one-to-one and onto. If there exist $x \neq y \in Y_U$ such that $\phi(x) = \phi(y)$, without loss of generality, assuming that there is a number n such that $x_n \neq y_n$ and $x_i = y_i$ for all $i < n$. This means that at state $x_{n-1} = y_{n-1}$ and $x_{n-2} = y_{n-2}$,

$$\Psi(x_{n-1}x_n) = 1 + \varphi(x_{n-1}) + 2\varphi(x_n) \neq 1 + \varphi(y_{n-1}) + 2\varphi(y_n) = \Psi(y_{n-1}y_n).$$

Therefore,

$$\Phi(x_{n-2}x_{n-1}x_n) = s_{\Psi(x_{n-2}x_{n-1})\Psi(x_{n-1}x_n)} \neq s_{\Psi(y_{n-2}y_{n-1})\Psi(y_{n-1}y_n)} = \Phi(y_{n-2}y_{n-1}y_n).$$

This contradicts to $\phi(x) = \phi(y)$. Thus, ϕ is one-to-one.

For every $s = (\cdots s_{i_{-1}i_0}s_{i_0i_1}s_{i_1i_2}\cdots) \in \mathbf{X}_{\mathcal{G}_\mathbf{S}}$, by (2.28) there exists a sequence $(\cdots k_{-1}k_0k_1\cdots)$ such that $t_{i_ji_{j+1};k_jk_{j+1}} \neq 0$ for all $j \in \mathbb{Z}$. By (2.16), the related pattern $\cdots x_{i_{-1}i_0;k_{-1}k_0}x_{i_0i_1;k_0k_1}x_{i_1i_2;k_1k_2}\cdots$ is admissible, i.e., $\begin{matrix}\cdots a_{r_{-1}}a_{r_0}a_{r_1}\cdots \\ \cdots a_{s_{-1}}a_{s_0}a_{s_1}\cdots\end{matrix}$ is admissible. By the definition of output space (2.14), the pattern $\cdots a_{r_{-1}}a_{r_0}a_{r_1}\cdots \in Y_U$. Moreover, by the relation in (2.12),

$$i_k = 1 + r_{k+1} + 2r_k, \quad \text{and} \quad r_k = \begin{cases} 1, & \text{if } a_{r_0} = +, \\ 0, & \text{if } a_{r_0} = -. \end{cases}$$

Hence, there exists $\cdots a_{r_{-1}}a_{r_0}a_{r_1}\cdots \in Y_U$ such that $\phi(\cdots a_{r_{-1}}a_{r_0}a_{r_1}\cdots) = s$. This shows that ϕ is onto, and the proof is completed. □

2.3.2. Entropy

Let $\Sigma_n(Y_U) \subseteq \{+,-\}^{\mathbb{Z}_{n\times 1}}$ denote the set of n-blocks in Y_U as in (2.24). The spatial entropy of Y_U is defined by

$$h(Y_U) = \lim_{n\to\infty} \frac{\log \Gamma_n(Y_U)}{n}, \tag{2.31}$$

where $\Gamma_n(Y_U)$ is the cardinal number of $\Sigma_n(Y_U)$. Example 2.5 demonstrates that Theorem 2.4 is invalid in computing the spatial entropy of Y_U. However, Theorem 2.13 shows that the output space Y_U is conjugate to the sofic shift $\mathbf{X}_{\mathcal{G}_\mathbf{S}}$. The entropy of Y_U can be computed by the following theorems show in [18].

Theorem 2.14. *(See [18].) If two shift spaces* $\mathbf{X}$ *and* $\mathbf{Y}$ *are conjugate, then* $h(\mathbf{X}) = h(\mathbf{Y})$.

Theorem 2.15. *(See [18].) Let* $\mathcal{G} = (G, \mathcal{L})$ *be a labeled graph. If* $\mathcal{G}$ *is right-resolving, then* $h(\mathbf{X}_\mathcal{G}) = h(\mathbf{X}_G)$.

Theorem 2.16. *For* Y_U *is given,* $\mathcal{G}_\mathbf{S}$ *is the sofic shift induced by* Y_U. *If* $\mathcal{G}_\mathbf{S}$ *is right-resolving, then* $h(Y_U) = \log \rho(\mathbf{T})$, *where* $\rho(\mathbf{T})$ *denotes the maximal eigenvalue of* $\mathbf{T}$.

Proof. Since Y_U is conjugate to $\mathbf{X}_{\mathcal{G}_\mathbf{S}}$, and $\mathcal{G}_\mathbf{S}$ is right-resolving, by Theorems 2.14, 2.15, and Perron–Frobenius theorem,

$$h(Y_U) = h(\mathbf{X}_{\mathcal{G}_\mathbf{S}}) = h(\mathbf{X}_\mathbf{T}) = \log \rho(\mathbf{T}). \tag{2.32}$$

This completes the proof. □

In general, $\mathcal{G}_\mathbf{S}$ induced by $Y_U(\mathcal{B})$ might not be right-resolving. However, a sofic shift $\mathcal{H} = (H, \mathcal{L}')$ which is right-resolving can be constructed and still conjugate to $Y_U(\mathcal{B})$ via the subset construction method stated in Section 2.2. Thus Theorem 2.16 can be extended to the general case.

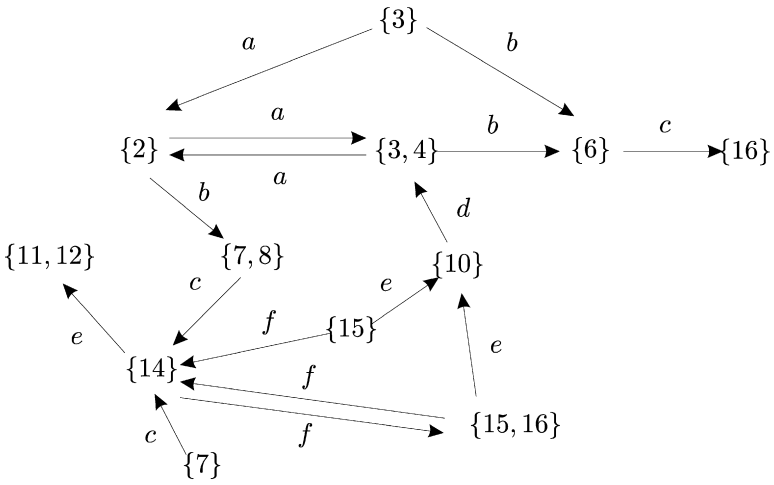

Fig. 2.4. A right-resolving labeled graph via subset construction.

Theorem 2.17. *For a given $\mathcal{B} \subseteq \{-,+\}^{\mathbb{Z}_{3\times 2}}$, let $Y_U \equiv Y_U(\mathcal{B})$ be the shift space induced by $\mathcal{B}$. Then there exists a labeled graph representation $\mathcal{H} = (H, \mathcal{L}')$ such that*

$$h(Y_U) = h(\mathbf{X}_{\mathcal{H}}) = \log \rho(\mathbf{H}). \tag{2.33}$$

Proof. For the admissible local patterns $\mathcal{B}$ given, let $\mathbf{T}$ and the labeled graph representation $\mathcal{G}_{\mathbf{S}}$ be defined as above. If $\mathcal{G}_{\mathbf{S}}$ is already right-resolving, then it is done. If not, using subset construction method, there is a labeled graph representation $\mathcal{H}$ such that $\mathbf{X}_{\mathcal{G}_{\mathbf{S}}} = \mathbf{X}_{\mathcal{H}}$ and is right-resolving. Note that the underlying graph and transition matrix of $\mathcal{H}$, H and $\mathbf{H}$, are also derived. Moreover, by Theorems 2.8 and 2.13, Y_U is conjugate to $\mathbf{X}_{\mathcal{H}}$. Thus, by Theorem 2.16, $h(Y_U) = h(\mathbf{X}_{\mathcal{H}}) = \log \rho(\mathbf{H})$. □

Example 2.18 *(Continued).* Let (A, B, z) be the same as in Example 2.5, $\mathcal{S} = \{s_{11}, s_{12}, s_{24}, s_{31}, s_{43}, s_{44}\}$, by (2.27), the symbolic transition matrix is

$$\mathbf{S} = \begin{pmatrix} s_{11}T_{11} & s_{12}T_{12} & 0 & 0 \\ 0 & 0 & 0 & s_{24}T_{24} \\ s_{31}T_{31} & 0 & 0 & 0 \\ 0 & 0 & s_{43}T_{43} & s_{44}T_{44} \end{pmatrix}. \tag{2.34}$$

Then, the labeled graph representation of $\mathcal{B}$, $\mathcal{G}_{\mathbf{S}} = (G_{\mathbf{T}}, \mathcal{L})$, is not right-resolving. For simplicity, denote the vertex set of $G_{\mathbf{T}}$ by $\mathcal{V} = \{1, 2, \ldots, 16\}$. Use the subset construction method to construct another labeled graph $\mathcal{H} = (H, \mathcal{L}')$ as in Fig. 2.4. Theorem 2.8 shows that $\mathbf{X}_{\mathcal{G}_{\mathbf{S}}} = \mathbf{X}_{\mathcal{H}}$.

The transition matrix of $\mathbf{X}_{\mathcal{H}}$ is obtained as below:

$$\mathbf{H} = \begin{pmatrix} 0 & 0 & 1 & 0 & 0 & 1 & 0 & 0 & 0 & 0 & 0 & 0 \\ 1 & 0 & 0 & 1 & 0 & 0 & 0 & 0 & 0 & 0 & 0 & 0 \\ 1 & 0 & 0 & 1 & 0 & 0 & 0 & 0 & 0 & 0 & 0 & 0 \\ 0 & 0 & 0 & 0 & 0 & 0 & 0 & 0 & 0 & 0 & 1 & 0 \\ 0 & 0 & 0 & 0 & 0 & 0 & 0 & 0 & 1 & 0 & 0 & 0 \\ 0 & 0 & 0 & 0 & 0 & 0 & 0 & 0 & 1 & 0 & 0 & 0 \\ 0 & 0 & 1 & 0 & 0 & 0 & 0 & 0 & 0 & 0 & 0 & 0 \\ 0 & 0 & 0 & 0 & 0 & 0 & 0 & 0 & 0 & 0 & 0 & 0 \\ 0 & 0 & 0 & 0 & 0 & 0 & 0 & 1 & 0 & 0 & 0 & 1 \\ 0 & 0 & 0 & 0 & 0 & 0 & 1 & 0 & 1 & 0 & 0 & 0 \\ 0 & 0 & 0 & 0 & 0 & 0 & 0 & 0 & 0 & 0 & 0 & 0 \\ 0 & 0 & 0 & 0 & 0 & 0 & 1 & 0 & 1 & 0 & 0 & 0 \end{pmatrix}. \tag{2.35}$$

Thus, $h((A, B, z); \mathcal{U}) = \log\lambda > 0$, where $\lambda \doteq 1.324718$ is the root of $f(t) = t^6 - 2t^4 + t^2 - 1$.

In the next subsection, the zeta function of Y_U will be discussed.

2.3.3. Zeta function

Given a sofic shift Y_U with shift map σ, invariant values and invariant functions of the shift space (Y_U, σ) are interested. In the last subsection, the entropy $h(\mathcal{B})$ is studied. This subsection examines the zeta function $\zeta_\sigma(t)$ with respect to the shift map σ.

Let $p_n(\sigma) = \{y = (y_i)_{i\in\mathbb{Z}} \in Y_U \mid \sigma^n(y) = y\}$ be the collection of all periodic patterns of period n. The zeta function of σ is defined as

$$\zeta_\sigma(t) = \exp\left(\sum_{n=1}^{\infty} \frac{p_n(\sigma)}{n} t^n\right), \tag{2.36}$$

where $\exp(x) = \sum_{n=0}^{\infty} \frac{x^n}{n!}$ is the classical exponential function.

If a shift space $\mathbf{X}$ is a shift of finite type, then there is an edge shift $\mathbf{X}_A$ conjugate to $\mathbf{X}$. The following theorem computes the zeta function of any shift of finite type.

Theorem 2.19. *(See [18].) Let A be a $k \times k$ nonnegative integer matrix, σ_A the associated shift map. Then*

$$\zeta_{\sigma_A}(t) = \frac{1}{\det(I_k - tA)}, \tag{2.37}$$

where I_k is the $k \times k$ identity matrix. Thus the zeta function of a shift of finite type is the reciprocal of a polynomial.

The following notations are needed to investigate the zeta function of sofic shift. Let $F = \{f_1, f_2, \ldots, f_m\}$ be a finite set. A permutation π of F is given below as an impression $(f_{i_1}, \ldots, f_{i_m})$, i.e., $\pi(f_\ell) = f_{i_\ell}$ for $1 \leqslant \ell \leqslant m$.

Definition 2.20. A permutation π is said to be even (odd, resp.) if the number of interchanges (or transpositions) needed to generate the permutation is even (odd, resp.) Moreover, the sign of π is defined as

$$\operatorname{sgn}(\pi) = \begin{cases} 1, & \pi \text{ is even,} \\ -1, & \pi \text{ is odd.} \end{cases} \tag{2.38}$$

Let $\mathcal{H} = (H, \mathcal{L}')$ be a labeled graph which is right-resolving with r many vertices, assuming that $\mathcal{V} = \{1, 2, \ldots, r\}$. Let $\mathbf{H}_S$ denote the symbolic transition matrix of $\mathcal{H}$ and $\mathbf{H}$ the transition matrix of the underlying graph H.

For $1 \leqslant k \leqslant r$, construct a labeled graph $\mathcal{H}_k$ with alphabet $\{\pm s_{ij} \colon s_{ij} \in \mathcal{S}\}$ as follows.

1. The vertex set of $\mathcal{H}_k$ is the set $\mathcal{V}_k$ of all subsets of $\mathcal{V}$ having k elements, i.e., $|\mathcal{V}_k| = \binom{r}{k}$. Moreover, the ordering on the states in each element of $\mathcal{V}_k$ is fixed.
2. For each $s_{ij} \in \mathcal{S}$, we denote $s_{ij}(I)$ the terminal state of s_{ij} starts at I. For $\mathcal{I} = \{I_1, \ldots, I_k\}, \mathcal{J} = \{J_1, \ldots, J_k\} \in \mathcal{V}_k$, there is an edge from $\mathcal{I}$ to $\mathcal{J}$ provided there exists $s_{ij} \in \mathcal{S}$ such that $s_{ij}(I_1), \ldots, s_{ij}(I_k)$ are well defined and $(s_{ij}(I_1), \ldots, s_{ij}(I_k))$ is a permutation of $\mathcal{J}$. More than this, the edge is labeled as s_{ij} ($-s_{ij}$, resp.) if the permutation is even (odd, resp.) Otherwise, there is no edge with label $\pm s_{ij}$ from $\mathcal{I}$ to $\mathcal{J}$.

Definition 2.21. Let $\mathbf{H}_{S_k}$ denote the symbolic transition matrix of $\mathcal{H}_k$, $\mathbf{H}_k$ be obtained from $\mathbf{H}_{S_k}$ by setting all the symbols in $\mathcal{S}$ equal to 1. We call $\mathbf{H}_k$ the kth signed subset matrix of $\mathcal{H}$.

Theorem 2.22. *(See [18].) Let $\mathcal{H} = (H, \mathcal{L}')$ be a right-resolving labeled graph with r many vertices, and $\mathbf{H}_k$ be its kth signed subset matrix. Then*

$$\zeta_{\sigma_{\mathcal{H}}}(t) = \prod_{k=1}^{r} \det(I - t\mathbf{H}_k)^{(-1)^k}, \tag{2.39}$$

where I is the identity matrix.

Theorem 2.23. *(See [18].) If two shift spaces $\mathbf{X}$ and $\mathbf{Y}$ are conjugate, then $\zeta_{\sigma_{\mathbf{X}}}(t) = \zeta_{\sigma_{\mathbf{Y}}}(t)$.*

Therefore, the zeta function of the sofic shift $\mathbf{X}_{\mathcal{G}_{\mathbf{S}}}$ can be derived using the following theorem.

Theorem 2.24. *For a given $\mathcal{B} \subseteq \{-, +\}^{\mathbb{Z}_{3\times 2}}$, let $Y_U \equiv Y_U(\mathcal{B})$ be the shift space induced by $\mathcal{B}$ with shift map σ. Then there exists a labeled graph representation $\mathcal{H}$ such that*

$$\zeta_{\sigma}(t) = \prod_{k=1}^{n} \det(I - t\mathbf{H}_k)^{(-1)^k}, \tag{2.40}$$

where $\mathbf{H}_k$ is the kth signed subset matrix of $\mathcal{H}$, and n is the cardinal number of the underlying graph H.

Proof. Let $\mathcal{G}_{\mathbf{S}}$ be the labeled graph representation of Y_U, and $\mathbf{X}_{\mathcal{G}_{\mathbf{S}}}$ be the sofic shift induced by $\mathcal{G}_{\mathbf{S}}$ with shift map $\sigma_{\mathcal{G}_{\mathbf{S}}}$. By Theorem 2.13, $\mathbf{X}_{\mathcal{G}_{\mathbf{S}}}$ is conjugate to Y_U. Thus, we have

$$\zeta_\sigma(t) = \zeta_{\sigma_{\mathcal{G}_{\mathbf{S}}}}(t). \tag{2.41}$$

If $\mathcal{G}_{\mathbf{S}}$ is right-resolving, then it is done by Theorem 2.22. Otherwise, construct a labeled graph $\mathcal{H}$ which is right-resolving and represents the same shift space as $\mathcal{G}_{\mathbf{S}}$ via subset construction method. This completes the proof. □

Example 2.25 *(Continued).* Continuing with Examples 2.5 and 2.18, for the investigation of zeta function, all the kth signed subset matrix $\mathbf{H}_k$ of $\mathcal{H}$ are needed to be constructed. Therefore, $\mathbf{H}_1 = \mathbf{H}$ as in (2.35),

$$\mathbf{H}_2 = \begin{pmatrix} 0 & -1 & -1 & 0 & 0 & 0 & 0 & 0 \\ 0 & -1 & -1 & 0 & 0 & 0 & 0 & 0 \\ 0 & 0 & 0 & 0 & -1 & 0 & 0 & 0 \\ 0 & 0 & 0 & 0 & -1 & 0 & 0 & 0 \\ 0 & 0 & 0 & 0 & 0 & 0 & 0 & 0 \\ 0 & 0 & 0 & 0 & 0 & 0 & -1 & -1 \\ 0 & 0 & 0 & 0 & 0 & 0 & -1 & -1 \\ 0 & 0 & 0 & 0 & 0 & 0 & 0 & 0 \end{pmatrix},$$

and $\mathbf{H}_3 = \mathbf{H}_4 = \cdots = \mathbf{H}_{12} = 0$, the zero matrix. Hence, by Theorem 2.22, $\zeta_\sigma(t) = \frac{(1+t)^2}{1-2t^2+t^4-t^6}$.

3. Multi-layer cellular neural networks

In this section, all results in one-layer CNN with input will be extended to multi-layer CNN.

3.1. Partition of parameter space

As in (1.1), an N-layer CNN system with input is of the form

$$\frac{dx_i^{(n)}}{dt} = -x_i^{(n)} + \sum_{|k|\leqslant d} a_k^{(n)} y_{i+k}^{(n)} + \sum_{|k|\leqslant d} b_k^{(n)} u_{i+k}^{(n)} + z^{(n)}, \tag{3.1}$$

for some $d \in \mathbb{N}$, $1 \leqslant n \leqslant N \in \mathbb{N}$, $i \in \mathbb{Z}$, where

$$u_i^{(n)} = y_i^{(n-1)} \quad \text{for } 2 \leqslant n \leqslant N, \qquad u_i^{(1)} = u_i, \qquad x_i(0) = x_i^0. \tag{3.2}$$

The feedback and controlling templates of each layer are

$$A^{(n)} = \big(a_{-d}^{(n)}, a_{-d+1}^{(n)}, \ldots, a_d^{(n)}\big) \quad \text{and} \quad B^{(n)} = \big(b_{-d}^{(n)}, b_{-d+1}^{(n)}, \ldots, b_d^{(n)}\big),$$

where $1 \leqslant n \leqslant N$. The parameter space and the admissible local patterns of each layer can be represented by $\mathcal{P}^{(n)} = \{(A^{(n)}, B^{(n)}, z^{(n)})\}$ and $\mathcal{B}^{(n)}(A^{(n)}, B^{(n)}, z^{(n)})$, where $1 \leqslant n \leqslant N$. Let $A = (A^{(1)}, A^{(2)}, \ldots, A^{(N)})$, $B = (B^{(1)}, B^{(2)}, \ldots, B^{(N)})$, $z = (z^{(1)}, z^{(2)}, \ldots, z^{(N)})$, $\mathcal{P}^m =$

$(\mathcal{P}^{(1)}, \mathcal{P}^{(2)}, \ldots, \mathcal{P}^{(N)})$, where $m = N(2d+1)-1$, $Y^{(n)} = y_{-d}^{(n)} y_{-d+1}^{(n)} \cdots y_{d}^{(n)}$, where $1 \leqslant n \leqslant N$, and $U = u_{-d} u_{-d+1} \cdots u_d$, then

$$\mathcal{B}(A, B, z) = \left\{ \begin{array}{l} Y^{(N)} \diamond Y^{(N-1)} \diamond \cdots \diamond Y^{(1)} \diamond U: \\ \quad Y^{(n)} \diamond Y^{(n-1)} \in \mathcal{B}^{(n)} \text{ for } 2 \leqslant n \leqslant N, \text{ and } Y^{(1)} \diamond U \in \mathcal{B}^{(1)} \end{array} \right\}, \tag{3.3}$$

where $\diamond$ is defined in (2.4). The generalized partition theorem of N-layer CNN then follows.

Theorem 3.1. *There exist $K(m) \in \mathbb{N}$ and unique collection of open subsets $\{P_k\}_{k=1}^{K(m)}$ of $\mathcal{P}^m$ such that*

(i) $\mathcal{P}^m = \bigcup_{k=1}^{K(m)} \overline{P}_k$;
(ii) $P_k \cap P_j = \emptyset$ *for* $k \neq j$;
(iii) $\mathcal{B}(A, B, z) = \mathcal{B}(\tilde{A}, \tilde{B}, \tilde{z}) \Leftrightarrow (A, B, z), (\tilde{A}, \tilde{B}, \tilde{z}) \in P_k$ *for some* k.

Proof. For simplicity, the case $N = 2$ is proved. The general case can be done analogously, the details are omitted here.

By Theorem 2.1, there exist $K_i \in \mathbb{N}$ and a unique collection of open subsets $\{P_k^{(i)}\}_{k=1}^{K_i}$ of $\mathcal{P}^{(i)}$ such that

(1) $\mathcal{P}_{(i)}^{4d+3} = \bigcup_{k=1}^{K_i} \overline{P_k^{(i)}}$;
(2) $P_k^{(i)} \cap P_\ell^{(i)} = \emptyset$ for $k \neq \ell$;
(3) $\mathcal{B}^{(i)}(A^{(i)}, B^{(i)}, z^{(i)}) = \mathcal{B}^{(i)}(\tilde{A}^{(i)}, \tilde{B}^{(i)}, \tilde{z}^{(i)})$ if and only if

$$\big(A^{(i)}, B^{(i)}, z^{(i)}\big), \big(\tilde{A}^{(i)}, \tilde{B}^{(i)}, \tilde{z}^{(i)}\big) \in P_k^{(i)} \quad \text{for some } k,$$

where $i = 1, 2$.

Let $K' = K_1 \cdot K_2$, define $P'_k = (P_{k_1}^{(1)}, P_{k_2}^{(2)})$, where $k = (k_1 - 1)K_2 + k_2$, $1 \leqslant k_1 \leqslant K_1$, $1 \leqslant k_2 \leqslant K_2$. Let

$$P_1 = P'_i, \quad \text{where } i = \min\big\{k \,\big|\, \text{there exist } Y^{(2)} \diamond Y^{(1)} \in \mathcal{B}^{(2)} \text{ and } Y^{(1)} \diamond U \in \mathcal{B}^{(1)}\big\}, \tag{3.4}$$

and

$$P_\ell = P'_i, \quad \text{where } i = \min_{k > k_{\ell-1}} \big\{k \,\big|\, \text{there exist } Y^{(2)} \diamond Y^{(1)} \in \mathcal{B}^{(2)} \text{ and } Y^{(1)} \diamond U \in \mathcal{B}^{(1)}\big\}, \tag{3.5}$$

for $\ell \geqslant 2$ and $k_j \in \mathbb{N}$ such that $P'_{k_j} = P_j$. Then there exists a positive integer $K \leqslant K'$ such that $\{P_k\}_{k=1}^{K}$ satisfies (i)–(iii), then the proof is completed. □

3.2. Ordering matrix

The ordering matrix $\mathbb{X}_{3\times N}$ of all possible local patterns in $\{+,-\}^{\mathbb{Z}_{3\times N}}$ is defined recursively as

$$\mathbb{X}_{3\times N}=\begin{bmatrix}\mathbf{X}_{11} & \mathbf{X}_{12} & \emptyset & \emptyset\\ \emptyset & \emptyset & \mathbf{X}_{23} & \mathbf{X}_{24}\\ \mathbf{X}_{31} & \mathbf{X}_{32} & \emptyset & \emptyset\\ \emptyset & \emptyset & \mathbf{X}_{43} & \mathbf{X}_{44}\end{bmatrix}, \tag{3.6}$$

where

$$\mathbf{X}_{i_1j_1}=\begin{bmatrix}X_{i_1j_1;11} & X_{i_1j_1;12} & \emptyset & \emptyset\\ \emptyset & \emptyset & X_{i_1j_1;23} & X_{i_1j_1;24}\\ X_{i_1j_1;31} & X_{i_1j_1;32} & \emptyset & \emptyset\\ \emptyset & \emptyset & X_{i_1j_1;43} & X_{i_1j_1;44}\end{bmatrix}, \tag{3.7}$$

$$\begin{aligned}&X_{i_1j_1;i_2j_2;\ldots;i_kj_k}\\ &=\begin{bmatrix}X_{i_1j_1;i_2j_2;\ldots;i_kj_k;11} & X_{i_1j_1;i_2j_2;\ldots;i_kj_k;12} & \emptyset & \emptyset\\ \emptyset & \emptyset & X_{i_1j_1;i_2j_2;\ldots;i_kj_k;23} & X_{i_1j_1;i_2j_2;\ldots;i_kj_k;24}\\ X_{i_1j_1;i_2j_2;\ldots;i_kj_k;31} & X_{i_1j_1;i_2j_2;\ldots;i_kj_k;32} & \emptyset & \emptyset\\ \emptyset & \emptyset & X_{i_1j_1;i_2j_2;\ldots;i_kj_k;43} & X_{i_1j_1;i_2j_2;\ldots;i_kj_k;44}\end{bmatrix},\end{aligned} \tag{3.8}$$

for $1\leqslant k\leqslant N-2$, and

$$\begin{aligned}&X_{i_1j_1;i_2j_2;\ldots;i_{N-1}j_{N-1}}\\ &=\begin{bmatrix}x_{i_1j_1;\ldots;i_{N-1}j_{N-1};11} & x_{i_1j_1;\ldots;i_{N-1}j_{N-1};12} & \emptyset & \emptyset\\ \emptyset & \emptyset & x_{i_1j_1;\ldots;i_{N-1}j_{N-1};23} & x_{i_1j_1;\ldots;i_{N-1}j_{N-1};24}\\ x_{i_1j_1;\ldots;i_{N-1}j_{N-1};31} & x_{i_1j_1;\ldots;i_{N-1}j_{N-1};32} & \emptyset & \emptyset\\ \emptyset & \emptyset & x_{i_1j_1;\ldots;i_{N-1}j_{N-1};43} & x_{i_1j_1;\ldots;i_{N-1}j_{N-1};44}\end{bmatrix},\end{aligned} \tag{3.9}$$

where $1\leqslant i_k,\ j_k\leqslant 4$, and $1\leqslant k\leqslant N$. The construction contains a self-similarity property in $\mathbb{X}_{3\times N}$. As in Section 2.1.2, $x_{i_1j_1;i_2j_2;\ldots;i_{N-1}j_{N-1};i_Nj_N}$ means the pattern

$$(a_{r_{11}r_{12}}a_{r'_{12}r_{13}})\diamond(a_{r_{21}r_{22}}a_{r'_{22}r_{23}})\diamond\cdots\diamond(a_{r_{N1}r_{N2}}a_{r'_{N2}r_{N3}})$$

in $\{+,-\}^{\mathbb{Z}_{3\times N}}$, where $a_{r_{k1}r_{k2}}a_{r'_{k2}r_{k3}}$ is defined in (2.10), and

$$r_{k1}=\left[\frac{i_k-1}{2}\right],\qquad r_{k2}=i_k-1-2r_{k1},\qquad r'_{k2}=\left[\frac{j_k-1}{2}\right],\qquad r_{k3}=j_k-1-2r'_{k2}.$$

The pattern is $\emptyset$ if $a_{r_{k1}r_{k2}}a_{r'_{k2}r_{k3}} = \emptyset$ for some $1 \leqslant k \leqslant N$. Otherwise, it is denoted by the pattern

$$(a_{r_{11}}a_{r_{12}}a_{r_{13}}) \diamond (a_{r_{21}}a_{r_{22}}a_{r_{23}}) \diamond \cdots \diamond (a_{r_{N1}}a_{r_{N2}}a_{r_{N3}})$$

in $\{+,-\}^{\mathbb{Z}_{3\times\infty}}$.

As long as the basic set of the admissible local patterns $\mathcal{B} \subseteq \{+,-\}^{\mathbb{Z}_{3\times(N+1)}}$ is given, $\Sigma_m(\mathcal{B})$ denotes the collection of all m-blocks generated by $\mathcal{B}$. The subshift space of $\{+,-\}^{\mathbb{Z}}$ is then defined by

$$Y_U = \left\{ \begin{array}{l} Y^{(N)} = (y_i^{(N)})_{i\in\mathbb{Z}}\text{: there exist } U, Y^{(1)}, Y^{(2)}, \ldots, Y^{(N-1)} \\ \quad \text{such that } Y^{(N)} \diamond Y^{(N-1)} \diamond \cdots \diamond Y^{(1)} \diamond U \in \Sigma(\mathcal{B}) \end{array} \right\}, \tag{3.10}$$

where $\Sigma(\mathcal{B}) \subseteq \{+,-\}^{\mathbb{Z}_{\infty\times(N+1)}}$ is generated by $\mathcal{B} \subseteq \{+,-\}^{\mathbb{Z}_{3\times(N+1)}}$.

3.3. Transition matrix

The basic set of admissible local patterns $\mathcal{B} = \mathcal{B}(A, B, z)$ can be determined from the N-layer CNN parameters (A, B, z). Denote by T_n the transition matrix induced by $\mathcal{B}^{(n)} \subseteq \{+,-\}^{\mathbb{Z}_{3\times 2}}$, where $\mathcal{B}^{(n)}$ is the basic set of admissible local patterns in the nth layer, and $1 \leqslant n \leqslant N$. Let $\hat{\mathbf{T}}_N = \mathbf{T}(\mathcal{B}; \mathcal{U})$ be the transition matrix induced by $\mathcal{B}$ with the set of input patterns $\mathcal{U}$. The following theorem is then obtained.

Theorem 3.2.

$$\hat{\mathbf{T}}_N = (T_N \otimes E_{4^{N-1}}) \circ (E_4 \otimes \overline{\mathbf{T}}_{N-1}) \in \mathcal{M}_{4^{n+1}\times 4^{n+1}}(\mathbb{R}), \tag{3.11}$$

where

$$\overline{\mathbf{T}}_n = (T_n \otimes E_{4^{n-1}}) \circ (E_4 \otimes \overline{\mathbf{T}}_{n-1}) \in \mathcal{M}_{4^{n+1}\times 4^{n+1}}(\mathbb{R}) \quad \textit{for } 2 \leqslant n \leqslant N-1, \tag{3.12}$$

and

$$\overline{\mathbf{T}}_1 = T_1 \circ (E_4 \otimes \mathbf{U}) \in \mathcal{M}_{16\times 16}(\mathbb{R}), \tag{3.13}$$

$\mathbf{U}$ *is the transition matrix of* $\mathcal{U}$. *Hence* $\overline{\mathbf{T}}_1$ *is the transition matrix given in Theorem* 2.3.

In particular, if $N = 2$,

$$\hat{\mathbf{T}}_2 = (T_2 \otimes E_4) \circ \big(E_4 \otimes \big(T_1 \circ (E_4 \otimes \mathbf{U})\big)\big). \tag{3.14}$$

Proof. For simplicity, the case $N = 2$ is proved. For $N \geqslant 2$, it can be done by mathematical induction, thus is omitted.

Denote $\hat{\mathbf{T}}_2 = (\hat{T}_{i_1 j_1})_{1\leqslant i_1, j_1 \leqslant 4}$ and $T_2 = (T_{i_1 j_1})_{1\leqslant i_1, j_1\leqslant 4}$, where $\hat{T}_{i_1 j_1} \in \mathcal{M}_{16\times 16}(\mathbb{R})$ and $T_{i_1 j_1} \in \mathcal{M}_{4\times 4}(\mathbb{R})$ for $1 \leqslant i_1, j_1 \leqslant 4$. The case $i_1 = j_1 = 1$ is proved, the others can be treated analogously.

Denote $\hat{T}_{11} = (\hat{T}_{11;i_2 j_2})_{1\leqslant i_2, j_2\leqslant 4}$, where $\hat{T}_{11;i_2 j_2} = (\hat{t}_{11;i_2 j_2;i_3 j_3})_{1\leqslant i_3, j_3\leqslant 4} \in \mathcal{M}_{4\times 4}(\mathbb{R})$, for fixed $1 \leqslant i_2, j_2 \leqslant 4$, and $T_{11} = (t_{11;i_2 j_2})_{1\leqslant i_2, j_2\leqslant 4} \in \mathcal{M}_{4\times 4}(\mathbb{R})$. Since the output patterns of the

first layer will be treated as the input patterns of the second layer, let $\mathcal{U}_2$ be the output patterns of the first layer coupled with input $\mathcal{U}$. By Theorem 2.3, the transition matrix of $\mathcal{U}_2$ is

$$\overline{\mathbf{T}}_1 = T_1 \circ (E_4 \otimes \mathbf{U}) \in \mathcal{M}_{16\times 16}(\mathbb{R}). \tag{3.15}$$

Denote

$$\overline{\mathbf{T}}_1 = (\overline{T}_{i_2 j_2})_{1\leqslant i_2, j_2\leqslant 4}, \quad \overline{T}_{i_2 j_2} = (\bar{t}_{i_2 j_2; i_3 j_3})_{1\leqslant i_3, j_3\leqslant 4} \in \mathcal{M}_{4\times 4}(\mathbb{R}). \tag{3.16}$$

Then

$$\hat{t}_{11; i_2 j_2; i_3 j_3} = 1 \quad \Leftrightarrow \quad t_{11; i_2 j_2} = 1 \quad \text{and} \quad \bar{t}_{i_2 j_2; i_3 j_3} = 1, \tag{3.17}$$

for $1 \leqslant i_2, j_2, i_3, j_3 \leqslant 4$. That is,

$$\hat{T}_{11} = (T_{11} \otimes E_4) \circ \big(T_1 \circ (E_4 \otimes \mathbf{U})\big). \tag{3.18}$$

The proof is completed. □

3.4. Entropy and zeta function

This subsection introduces the formula for calculating entropy and zeta function of N-layer CNN. Let $\mathcal{S}^{(n)} = \{s_{ij}^{(n)}\}_{1\leqslant i,j\leqslant 4}$ be the alphabets, and let $\mathbf{S}_n$ and $\mathbf{S}$ be the symbolic transition matrices of T_n over $\mathcal{S}^{(n)}$ and $\hat{\mathbf{T}}_N$ for $1 \leqslant n \leqslant N$. By Theorem 2.9, $\mathbf{X}_{\mathcal{G}_{\mathbf{S}_n}}$ is a sofic shift induced by $\mathcal{B}^{(n)}$, where $\mathcal{G}_{\mathbf{S}_n}$ is the labeled graph representation of the nth layer. Furthermore, Y_U is the output space induced by the N-layer CNN as defined in (3.10). The following theorem can be obtained by the same method in Theorem 2.13, so the details are omitted.

Theorem 3.3. *Y_U is conjugate to $\mathbf{X}_{\mathcal{G}_{\mathbf{S}}}$.*

The definition of convolution is given below.

Definition 3.4. Let $\mathbf{X}, \mathbf{Y}$ be two shift spaces with graph representation $G_{\mathbf{X}} = (\mathcal{V}_{\mathbf{X}}, \mathcal{E}_{\mathbf{X}})$, $G_{\mathbf{Y}} = (\mathcal{V}_{\mathbf{Y}}, \mathcal{E}_{\mathbf{Y}})$, resp., then the convolution of $\mathbf{X}, \mathbf{Y}$, denoted by $\mathbf{X} * \mathbf{Y}$, is the shift space with underlying graph $G_{\mathbf{X}*\mathbf{Y}} = (\mathcal{V}_{\mathbf{X}*\mathbf{Y}}, \mathcal{E}_{\mathbf{X}*\mathbf{Y}})$, where

$$\mathcal{V}_{\mathbf{X}*\mathbf{Y}} = \big\{ f(x) \in \mathcal{E}_{\mathbf{Y}} \,\big|\, x \in \mathcal{V}_{\mathbf{X}} \big\} \tag{3.19}$$

for some $f : \mathcal{V}_{\mathbf{X}} \to \mathcal{E}_{\mathbf{Y}}$.

The convolution theorem for an N-many sofic shift is then obtained.

Theorem 3.5. *Let $\mathbf{X}_{\mathcal{G}_{\mathbf{S}}}$ be the sofic shift induced by $\mathcal{B}$, then*

$$\mathbf{X}_{\mathcal{G}_{\mathbf{S}}} = \mathbf{X}_{\mathcal{G}_{\mathbf{S}_N}} * \cdots * \mathbf{X}_{\mathcal{G}_{\mathbf{S}_2}} * \mathbf{X}_{\mathcal{G}_{\mathbf{S}_1}} \tag{3.20}$$

is the convolution of $\mathbf{X}_{\mathcal{G}_{\mathbf{S}_1}}, \ldots, \mathbf{X}_{\mathcal{G}_{\mathbf{S}_N}}$,

$$\hat{\mathbf{S}}_N = (\mathbf{S}_N \otimes E_{4^{N-1}}) \circ (E_4 \otimes \bar{\mathbf{S}}_{N-1}), \tag{3.21}$$

where

$$\bar{\mathbf{S}}_n = (\mathbf{S}_n \otimes E_{4^{n-1}}) \circ (E_4 \otimes \bar{\mathbf{S}}_{n-1}) \in \mathcal{M}_{4^{n+1}\times 4^{n+1}}(\mathbb{R}) \quad \text{for } 2 \leqslant n \leqslant N-1, \tag{3.22}$$

and

$$\bar{\mathbf{S}}_1 = \mathbf{S}_1 \circ (E_4 \otimes \mathbf{U}) \in \mathcal{M}_{16}(\mathbb{R}). \tag{3.23}$$

Proof. This can be done using the same method used in the proof of Theorem 3.2, the details are omitted. □

Thus, the theorems for entropy and zeta function can be found via the same methods as described in the last section.

Theorem 3.6. *For a given* $\mathcal{B} \subseteq \{+,-\}^{\mathbb{Z}_{3\times(N+1)}}$, *let* $Y_U \equiv Y_U(\mathcal{B})$ *be the shift space induced by* $\mathcal{B}$. *Then there exists a labeled graph representation* $\mathcal{H} = (H, \mathcal{L}')$ *such that*

$$h(Y_U) = h(\mathbf{X}_{\mathcal{H}}) = \log \rho(\mathbf{H}), \tag{3.24}$$

and

$$\zeta_\sigma(t) = \prod_{k=1}^{r} \det(I - t\mathbf{H}_k)^{(-1)^k}, \tag{3.25}$$

where $\mathbf{H}_k$ *is the* k*th signed subset matrix of* $\mathcal{H}$, *and* r *is the cardinal number of the underlying graph* H.

An example for 2-layer CNN is illustrated here.

Example 3.7. Consider (A, B, z) with $A^{(1)} = A^{(2)} \equiv \overline{A}$, $B^{(1)} = B^{(2)} \equiv \overline{B}$, $z^{(1)} = z^{(2)} \equiv \bar{z}$, and $\overline{A}$, $\overline{B}$ and $\bar{z}$ satisfy the same condition described in Example 2.5. Moreover, the set of input patterns is given by $\mathcal{U} = \{-+-, -++, +-+\}$. Then $\mathcal{B}^{(1)} = \mathcal{B}(A^{(1)}, B^{(1)}, z^{(1)}; \mathcal{U})$ consists of the following patterns:

$$\begin{array}{cccc}
\begin{matrix} - & \ominus & - \\ - & \boxplus & - \end{matrix} &
\begin{matrix} - & \ominus & - \\ - & \boxplus & + \end{matrix} &
\begin{matrix} - & \ominus & - \\ + & \boxminus & + \end{matrix} &
\begin{matrix} - & \ominus & + \\ - & \boxplus & - \end{matrix} \\
\begin{matrix} - & \ominus & + \\ - & \boxplus & + \end{matrix} &
\begin{matrix} - & \ominus & + \\ + & \boxminus & + \end{matrix} &
\begin{matrix} + & \ominus & - \\ - & \boxplus & - \end{matrix} &
\begin{matrix} + & \ominus & - \\ - & \boxplus & + \end{matrix} \\
\begin{matrix} + & \oplus & + \\ + & \boxminus & + \end{matrix} &
\begin{matrix} + & \oplus & + \\ - & \boxplus & + \end{matrix} &
\begin{matrix} + & \oplus & + \\ - & \boxplus & - \end{matrix} &
\begin{matrix} + & \oplus & - \\ + & \boxminus & + \end{matrix} \\
\begin{matrix} + & \oplus & - \\ - & \boxplus & + \end{matrix} &
\begin{matrix} + & \oplus & - \\ - & \boxplus & - \end{matrix} &
\begin{matrix} - & \oplus & + \\ + & \boxminus & + \end{matrix} &
\begin{matrix} - & \oplus & + \\ - & \boxplus & + \end{matrix}
\end{array}$$

Denote $\mathcal{U}_2$ the output patterns of $\mathcal{B}^{(1)}$, i.e.,

$$\mathcal{U}_2 = \{---, --+, +--, +++, ++-, -++\}.$$

Then $\mathcal{B}^{(2)} = \mathcal{B}(A^{(2)}, B^{(2)}, z^{(2)}; \mathcal{U}_2)$ consists of the following patterns:

$$\begin{array}{cccc}
\begin{matrix} + & \oplus & + \\ + & \boxplus & + \end{matrix} &
\begin{matrix} + & \oplus & + \\ + & \boxplus & - \end{matrix} &
\begin{matrix} + & \oplus & + \\ + & \boxminus & - \end{matrix} &
\begin{matrix} + & \oplus & - \\ + & \boxplus & + \end{matrix} \\
\begin{matrix} + & \oplus & - \\ + & \boxplus & - \end{matrix} &
\begin{matrix} + & \oplus & + \\ - & \boxplus & + \end{matrix} &
\begin{matrix} + & \oplus & - \\ + & \boxminus & - \end{matrix} &
\begin{matrix} - & \oplus & + \\ + & \boxplus & + \end{matrix} \\
\begin{matrix} + & \oplus & + \\ - & \boxminus & + \end{matrix} &
\begin{matrix} - & \oplus & + \\ + & \boxplus & - \end{matrix} &
\begin{matrix} + & \oplus & - \\ - & \boxminus & - \end{matrix} &
\begin{matrix} + & \oplus & - \\ - & \boxplus & + \end{matrix} \\
\begin{matrix} - & \oplus & + \\ + & \boxminus & - \end{matrix} &
\begin{matrix} - & \oplus & - \\ + & \boxplus & + \end{matrix} &
\begin{matrix} + & \oplus & - \\ - & \boxminus & + \end{matrix} &
\begin{matrix} - & \oplus & - \\ + & \boxplus & - \end{matrix} \\
\begin{matrix} + & \oplus & - \\ - & \boxminus & - \end{matrix} &
\begin{matrix} - & \oplus & + \\ - & \boxplus & + \end{matrix} &
\begin{matrix} - & \ominus & - \\ - & \boxminus & - \end{matrix} &
\begin{matrix} - & \ominus & - \\ - & \boxminus & + \end{matrix} \\
\begin{matrix} - & \ominus & - \\ - & \boxplus & + \end{matrix} &
\begin{matrix} - & \ominus & + \\ - & \boxminus & - \end{matrix} &
\begin{matrix} - & \ominus & + \\ - & \boxminus & + \end{matrix} &
\begin{matrix} - & \ominus & - \\ + & \boxminus & - \end{matrix} \\
\begin{matrix} - & \ominus & + \\ - & \boxplus & + \end{matrix} &
\begin{matrix} + & \ominus & - \\ - & \boxminus & - \end{matrix} &
\begin{matrix} - & \ominus & - \\ + & \boxplus & - \end{matrix} &
\begin{matrix} + & \ominus & - \\ - & \boxminus & + \end{matrix} \\
\begin{matrix} - & \ominus & - \\ + & \boxplus & + \end{matrix} &
\begin{matrix} - & \ominus & + \\ + & \boxminus & - \end{matrix} &
\begin{matrix} + & \ominus & - \\ - & \boxplus & + \end{matrix} &
\end{array}$$

The transition matrix $\hat{\mathbf{T}} = \mathbf{T}((A, B, z); \mathcal{U})$ is then

$$\hat{\mathbf{T}} = \begin{pmatrix} \hat{\mathbf{T}}_{11} & \hat{\mathbf{T}}_{12} & 0 & 0 \\ 0 & 0 & \hat{\mathbf{T}}_{23} & \hat{\mathbf{T}}_{24} \\ \hat{\mathbf{T}}_{31} & 0 & 0 & 0 \\ 0 & 0 & \hat{\mathbf{T}}_{43} & \hat{\mathbf{T}}_{44} \end{pmatrix}, \tag{3.26}$$

where

$$\hat{\mathbf{T}}_{11} = \hat{\mathbf{T}}_{43} = \hat{\mathbf{T}}_{44} = \begin{pmatrix} T_1 & T_1 & 0 & 0 \\ 0 & 0 & 0 & T_3 \\ T_2 & 0 & 0 & 0 \\ 0 & 0 & T_1 & T_1 \end{pmatrix}, \qquad \hat{\mathbf{T}}_{12} = \begin{pmatrix} T_1 & T_1 & 0 & 0 \\ 0 & 0 & 0 & T_3 \\ T_2 & 0 & 0 & 0 \\ 0 & 0 & 0 & 0 \end{pmatrix},$$

$$\hat{\mathbf{T}}_{23} = \begin{pmatrix} 0 & 0 & 0 & 0 \\ 0 & 0 & 0 & 0 \\ 0 & 0 & 0 & 0 \\ 0 & 0 & T_1 & T_1 \end{pmatrix}, \qquad \hat{\mathbf{T}}_{24} = \begin{pmatrix} 0 & 0 & 0 & 0 \\ 0 & 0 & 0 & T_3 \\ T_2 & 0 & 0 & 0 \\ 0 & 0 & T_1 & T_1 \end{pmatrix}, \qquad \hat{\mathbf{T}}_{31} = \begin{pmatrix} T_1 & T_1 & 0 & 0 \\ 0 & 0 & 0 & T_3 \\ 0 & 0 & 0 & 0 \\ 0 & 0 & 0 & 0 \end{pmatrix},$$

and

$$T_1 = \begin{pmatrix} 0 & 0 & 0 & 0 \\ 0 & 0 & 1 & 1 \\ 0 & 1 & 0 & 0 \\ 0 & 0 & 0 & 0 \end{pmatrix}, \qquad T_2 = \begin{pmatrix} 0 & 0 & 0 & 0 \\ 0 & 0 & 1 & 1 \\ 0 & 0 & 0 & 0 \\ 0 & 0 & 0 & 0 \end{pmatrix}, \qquad T_3 = \begin{pmatrix} 0 & 0 & 0 & 0 \\ 0 & 0 & 0 & 1 \\ 0 & 1 & 0 & 0 \\ 0 & 0 & 0 & 0 \end{pmatrix}.$$

Table 3.1
Some maximal eigenvalues produced in one-layer CNN with input

Maximal eigenvalue	Characteristic polynomial
$\lambda_1 = 2$	$t - 2$
$\lambda_2 \doteq 1.9479$	$t^5 - 2t^4 + t^3 - 2t^2 + t - 1$
$\lambda_3 \doteq 1.8832$	$t^4 - 2t^3 + t^2 - 2t + 1$
$\lambda_4 \doteq 1.8393$	$t^3 - t^2 - t + 1$
$\lambda_5 \doteq 1.7549$	$t^3 - 2t^2 + t - 1$
$\lambda_6 \doteq 1.7417$	$t^8 - 2t^7 + t^6 - t^5 + t^4 - 2t^3 + t^2 - 1$
$\lambda_7 \doteq 1.6992$	$t^5 - 2t^4 + t^3 - 2t + 1$
$\lambda_8 = g \doteq 1.618$	$t^2 - t - 1$
$\lambda_9 \doteq 1.5618$	$t^6 - 2t^5 + t^4 - t^2 + t - 1$
$\lambda_{10} \doteq 1.5289$	$t^5 - 2t^4 + t^3 - 1$

Let $\mathcal{S} = \{s_{11}, s_{12}, s_{23}, s_{24}, s_{31}, s_{43}, s_{44}\}$, the symbolic transition matrix is

$$\mathbf{S} = \begin{pmatrix} s_{11}\hat{\mathbf{T}}_{11} & s_{12}\hat{\mathbf{T}}_{12} & 0 & 0 \\ 0 & 0 & s_{23}\hat{\mathbf{T}}_{23} & s_{24}\hat{\mathbf{T}}_{24} \\ s_{31}\hat{\mathbf{T}}_{31} & 0 & 0 & 0 \\ 0 & 0 & s_{43}\hat{\mathbf{T}}_{43} & s_{44}\hat{\mathbf{T}}_{44} \end{pmatrix}, \tag{3.27}$$

which is not right-resolving. Using subset construction method, the spatial entropy then can be found, $h((A, B, z); \mathcal{U}) = \log\lambda$, where $\lambda \doteq 1.49676$ is a root of $f(t) = t^8 - 2t^6 + t^4 - 3t^2 - 1$. Moreover, the zeta function is

$$\zeta_\sigma(t) = \frac{(1 + t + t^3)(1 + t - t^3)}{1 - 2t^2 + t^4 - 3t^6 - t^8}.$$

3.5. The broken of symmetry

The basic set of admissible local patterns $\mathcal{B}$ can be determined from (A, B, z). The entropy of each partition is symmetrical in one-dimensional CNN without input, i.e., where $B \equiv 0$ [15]. For example, if (A, z) is picked such that $a_l > a_r > 0$, then parameters a and z have 25 regions. Clearly,

$$h\big(\mathcal{B}\big([m, n]\big)\big) = h\big(\mathcal{B}\big([n, m]\big)\big) \quad \text{for } 1 \leqslant m, n \leqslant 4. \tag{3.28}$$

The symmetry is broken for the one-layer CNN with input, as shown below with an example. Consider

$$\frac{dx_i}{dt} = -x_i + a_l y_{i-1} + a y_i + a_r y_{i+1} + b_l u_{i-1} + b u_i + b_r u_{i+1} + z, \tag{3.29}$$

where $b_l = 0$, then the symmetry of entropy is broken, as revealed in Fig. 3.1.

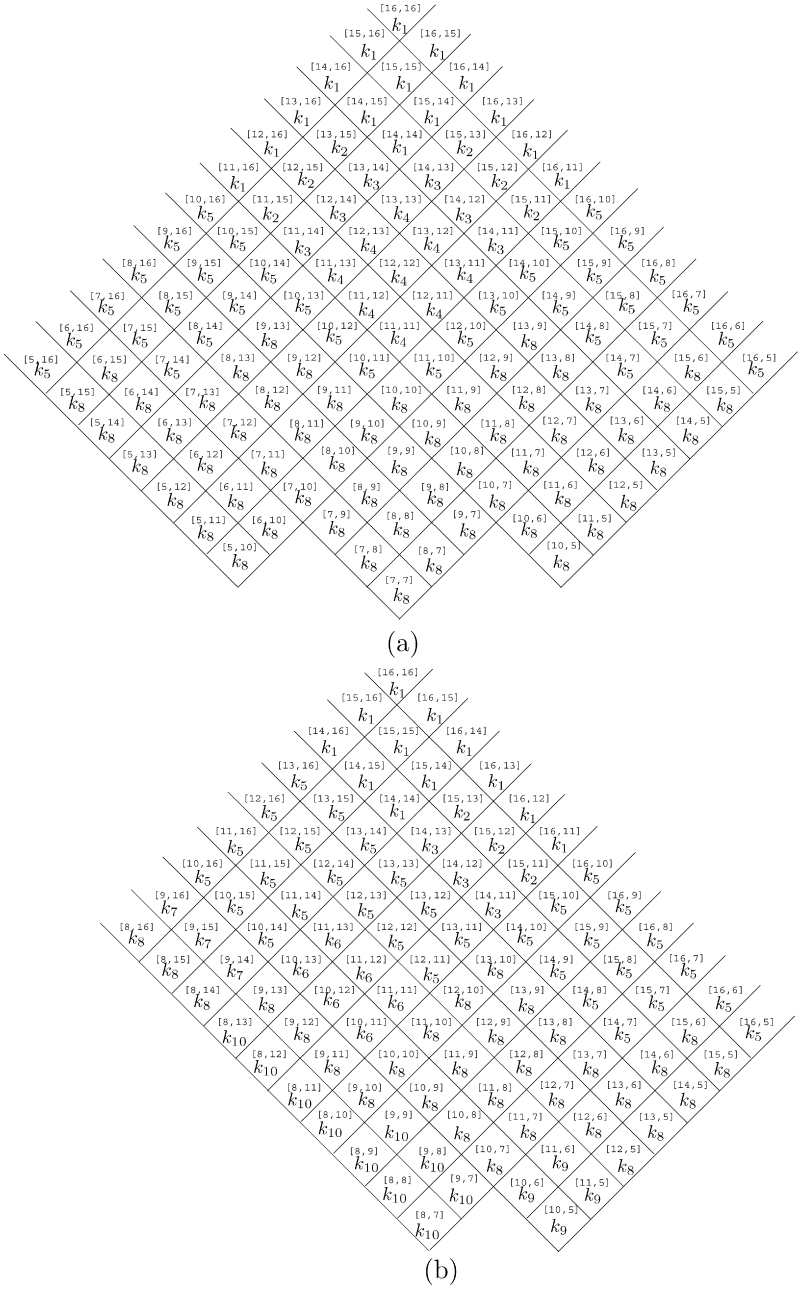

Fig. 3.1. The effect of input patterns. The parameters a_l, a_r, b, b_r are considered as follows. (i) $a_l > a_r > b > b_r > 0$, (ii) $a_l < b + b_r$, (iii) $a_l + b_r < a_r + b$. Subfigure (a) lists regions that produce positive entropy. Those regions with positive entropy are symmetric, i.e., $h([m,n]) = h([n,m])$. However, such property would be destroyed when input patterns are given. Subfigure (b) lists the same regions as in (a) but the input patterns $\mathcal{U} = \{--, -+, +-\}$ are considered. It is seen that the symmetry is no longer hold. Herein, $k_i = \log \lambda_i$ for $1 \leqslant i \leqslant 10$ are listed in Table 3.1.

Appendix A

This appendix introduces in detail the relationship between the admissible local patterns and the partition of parameter space in Example 2.5. A one-dimensional CNN with input is of the form

$$\frac{dx_i}{dt} = -x_i + a_l y_{i-1} + a y_i + a_r y_{i+1} + b_l u_{i-1} + b u_i + b_r u_{i+1} + z, \tag{A.1}$$

where $A = [a_l, a, a_r]$, $B = [b_l, b, b_r]$ represent the feedback and controlling templates, respectively; $y = f(x) = \frac{1}{2}(|x+1| - |x-1|)$ is the output function, and z is the threshold.

Consider that a_l, a_r, b_l, b, b_r satisfies the inequality in Example 2.5, i.e., the partition for the parameter space $\{(a_l, a_r, b_l, b, b_r)\}$ is chosen. For a given mosaic solution $\bar{x}$, the state at cell C_i is $+$, i.e., $\bar{x}_i > 1$, if and only if

$$a - 1 + z > -(a_l y_{i-1} + a_r y_{i+1} + b u_i + b_r u_{i+1}). \tag{A.2}$$

Similarly, the state at cell C_i is $-$, i.e., $\bar{x}_i < -1$, if and only if

$$a - 1 - z > a_l y_{i-1} + a_r y_{i+1} + b u_i + b_r u_{i+1}. \tag{A.3}$$

Let $\alpha = (a_l, a_r)$, $\beta = (b_l, b, b_r)$, $V^n = \{v = (v_i) \in \mathbb{R}^n\colon\ |v_i| = 1 \text{ for all } 1 \leqslant i \leqslant n\}$, the basic set of admissible local patterns with "+" state in the center is defined as

$$\mathcal{B}(+, A, B, z) = \big\{v \diamond w\colon\ a - 1 + z > -(\alpha \cdot v + \beta \cdot w)\big\}, \tag{A.4}$$

where $v \in V^2$ and $w \in V^3$. Similarly, the basic set of admissible local patterns with "$-$" state in the center is defined as

$$\mathcal{B}(-, A, B, z) = \{v' \diamond w'\colon\ a - 1 - z > \alpha \cdot v' + \beta \cdot w'\}. \tag{A.5}$$

Furthermore, the basic set of admissible local patterns derived from (A, B, z) is denoted by

$$\mathcal{B}(A, B, z) = \big(\mathcal{B}(+, A, B, z), \mathcal{B}(-, A, B, z)\big). \tag{A.6}$$

Let ℓ_i^+, ℓ_j^- denote the linear maps

$$a - 1 + z = c_i^+ \quad \text{and} \quad a - 1 - z = c_j^-$$

for some c_i^+, c_j^-, $1 \leqslant i, j \leqslant 32$, respectively. By the conditions (i)–(iv) in Example 2.5, the following relation can be obtained:

$$c_1^- < c_2^- < \cdots < c_{16}^- < 0 < c_{17}^- < c_{18}^- < \cdots < c_{32}^-, \tag{A.7}$$

and $c_k^- = -c_{33-k}^+$, $1 \leqslant k \leqslant 32$, where

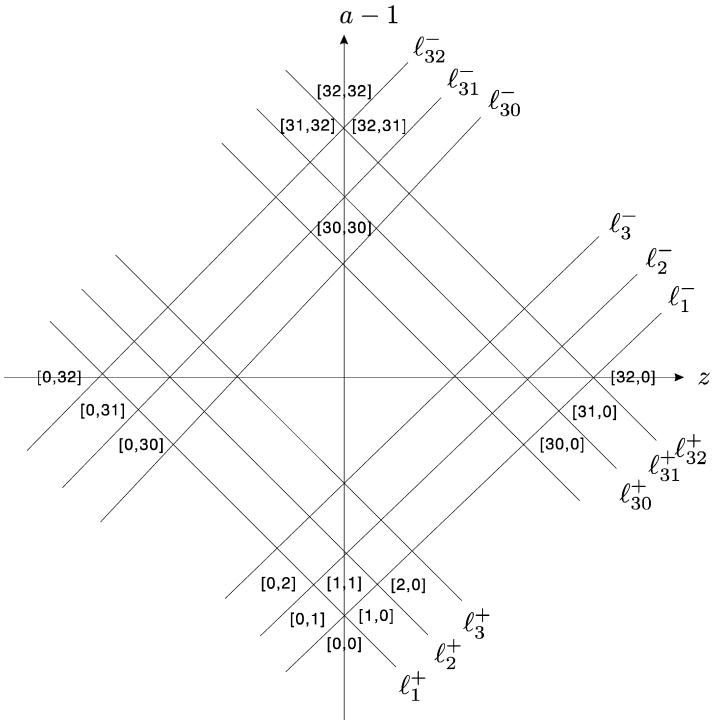

Fig. A.1. The $(a-1, z)$ bifurcation diagram.

$$
\begin{aligned}
c_1^- &= -a_l - a_r - b_l - b - b_r, & c_{17}^- &= a_l - a_r - b_l + b - b_r,\\
c_2^- &= -a_l - a_r - b_l - b + b_r, & c_{18}^- &= a_l - a_r - b_l + b + b_r,\\
c_3^- &= -a_l - a_r - b_l + b - b_r, & c_{19}^- &= a_l + a_r - b_l - b - b_r,\\
c_4^- &= -a_l - a_r - b_l + b + b_r, & c_{20}^- &= -a_l + a_r + b_l + b - b_r,\\
c_5^- &= -a_l + a_r - b_l - b - b_r, & c_{21}^- &= a_l + a_r - b_l - b + b_r,\\
c_6^- &= -a_l + a_r - b_l - b + b_r, & c_{22}^- &= -a_l + a_r + b_l + b + b_r,\\
c_7^- &= -a_l - a_r + b_l - b - b_r, & c_{23}^- &= a_l - a_r + b_l - b - b_r,\\
c_8^- &= -a_l - a_r + b_l - b + b_r, & c_{24}^- &= a_l - a_r + b_l - b + b_r,\\
c_9^- &= -a_l + a_r - b_l + b - b_r, & c_{25}^- &= a_l + a_r - b_l + b - b_r,\\
c_{10}^- &= -a_l + a_r - b_l + b + b_r, & c_{26}^- &= a_l + a_r - b_l + b + b_r,\\
c_{11}^- &= a_l - a_r - b_l - b - b_r, & c_{27}^- &= a_l - a_r + b_l + b - b_r,\\
c_{12}^- &= -a_l - a_r + b_l + b - b_r, & c_{28}^- &= a_l - a_r + b_l + b + b_r,\\
c_{13}^- &= a_l - a_r - b_l - b + b_r, & c_{29}^- &= a_l + a_r + b_l - b - b_r,\\
c_{14}^- &= -a_l - a_r + b_l + b + b_r, & c_{30}^- &= a_l + a_r + b_l - b + b_r,\\
c_{15}^- &= -a_l + a_r + b_l - b - b_r, & c_{31}^- &= a_l + a_r + b_l + b - b_r,\\
c_{16}^- &= -a_l + a_r + b_l - b + b_r, & c_{32}^- &= a_l + a_r + b_l + b + b_r.
\end{aligned}
$$

Fig. A.1 depicts a bifurcation diagram of the $(a-1, z)$ parameter space. The basic set of admissible local patterns is then determined once the parameters a and z are chosen, i.e., some specified

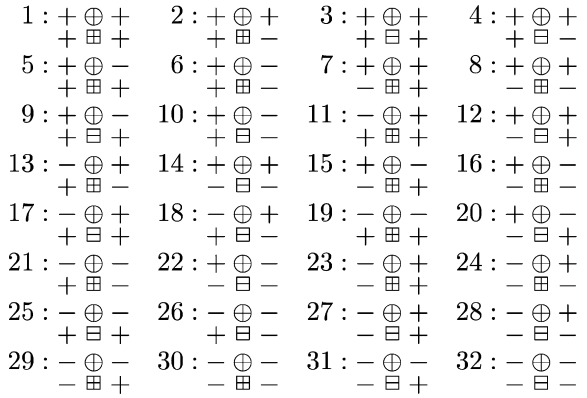

Fig. A.2. The order of the appearance of the patterns with state "+" in the center.

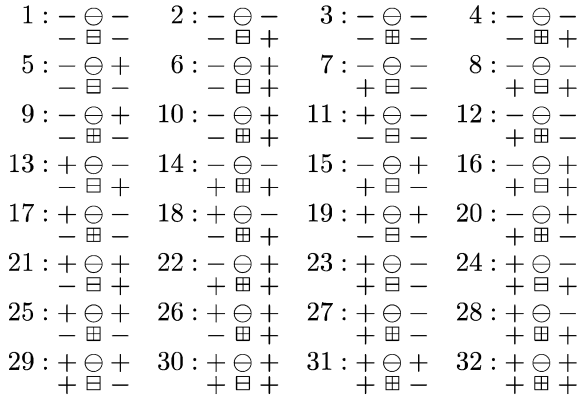

Fig. A.3. The order of the appearance of the patterns with state "−" in the center.

region in the bifurcation diagram is selected. More precisely, if a region $[m, n]$ in the bifurcation diagram has been chosen, then for $y \diamond u \in \mathcal{B}(+, A, B, z)$, the admissible local pattern with state "+" in the center, $y \diamond u$ satisfies the following inequalities:

$$a - 1 + z > -(\alpha \cdot y + \beta \cdot u), \tag{A.8}$$

$$c_m^+ < a - 1 + z < c_{m+1}^+. \tag{A.9}$$

Similarly, for $y' \diamond u' \in \mathcal{B}(-, A, B, z)$, $y' \diamond u'$ satisfies the following inequalities:

$$a - 1 - z > \alpha \cdot y' + \beta \cdot u', \tag{A.10}$$

$$c_n^- < a - 1 - z < c_{n+1}^-. \tag{A.11}$$

In other words, m patterns have the center state "+", and n patterns have the center state "−". The chosen partition uniquely determines the order of those patterns. Fig. A.2 lists the order of the patterns with "+" in the center. Fig. A.3 lists the order of the patterns with "−" in the center.

References

[1] J.C. Ban, W.G. Hu, S.S. Lin, Y.H. Lin, Zeta functions for two-dimensional subshift of finite type, preprint, 2007.
[2] J.C. Ban, S.S. Lin, Patterns generation and transition matrices in multi-dimensional lattice models, Discrete Contin. Dyn. Syst. 13 (2005) 637–658.
[3] J.-C. Ban, S.-S. Lin, Y.-H. Lin, Patterns generation and spatial entropy in two-dimensional lattice models, Asian J. Math. 11 (3) (2007) 497–534.
[4] J.C. Ban, S.S. Lin, Y.H. Lin, Three-dimensional cellular neural networks and patterns generation problems, Internat. J. Bifur. Chaos Appl. Sci. Engrg. (2008), in press.
[5] J.C. Ban, S.S. Lin, Y.H. Lin, Primitivity of subshifts of finite type in two-dimensional lattice models, preprint, 2007.
[6] S.N. Chow, J. Mallet-Paret, E.S. Van Vleck, Pattern formation and spatial chaos in spatially discrete evolution equations, Random Comput. Dynam. 4 (1996) 109–178.
[7] L.O. Chua, CNN: A Paradigm for Complexity, World Sci. Ser. Nonlinear Sci. Ser. A, vol. 31, World Scientific, Singapore, 1998.
[8] L.O. Chua, L. Yang, Cellular neural networks: Theory, IEEE Trans. Circuits Syst. I Regul. Pap. 35 (1988) 1257–1272.
[9] L.O. Chua, L. Yang, Cellular neural networks: Applications, IEEE Trans. Circuits Syst. I Regul. Pap. 35 (1988) 1273–1290.
[10] G.B. Ermentrout, Stable periodic solutions to discrete and continuum arrays of weakly coupled nonlinear oscillators, SIAM J. Appl. Math. 52 (1992) 1665–1687.
[11] G.B. Ermentrout, N. Kopell, Inhibition-produced patterning in chains of coupled nonlinear oscillators, SIAM J. Appl. Math. 54 (1994) 478–507.
[12] G.B. Ermentrout, N. Kopell, T.L. Williams, On chains of oscillators forced at one end, SIAM J. Appl. Math. 51 (1991) 1397–1417.
[13] T. Eveneux, J.P. Laplante, Propagation failure in arrays of coupled bistable chemical reactors, J. Phys. Chem. 96 (1992) 4931–4934.
[14] C.H. Hsu, J. Juang, S.S. Lin, W.W. Lin, Cellular neural networks: Local patterns for general template, Internat. J. Bifur. Chaos Appl. Sci. Engrg. 10 (2000) 1645–1659.
[15] J. Juang, S.S. Lin, Cellular neural networks: Mosaic pattern and spatial chaos, SIAM J. Appl. Math. 60 (2000) 891–915.
[16] J.P. Keener, Propagation and its failure in coupled systems of discrete excitable cells, SIAM J. Appl. Math. 47 (1987) 556–572.
[17] J.P. Keener, The effects of discrete gap junction coupling on propagation in myocardium, J. Theoret. Biol. 148 (1991) 49–82.
[18] D. Lind, B. Marcus, An Introduction to Symbolic Dynamics and Coding, Cambridge Univ. Press, Cambridge, 1995.
[19] C.W. Shih, Influence of boundary conditions on pattern formation and spatial chaos in lattice systems, SIAM J. Appl. Math. 61 (2000) 335–368.